Lecture at 1st Summer School at Forschungszentrum Jülich, September 2002
Published in: "Polarized Neutron Scattering", Th. Brückel, W.Schweika, eds.,
Series "Matter and Materials", Vol.12, p. 247.

9 Polarized Neutron Reflection and Off-Specular Scattering

Boris P. TOPERVERG

Institut für Festkörperforschung, Forschungszentrum Jülich, Germany
Petersburg Nuclear Physics Institute, Gatchina, 188300 St. Petersburg, Russia

A theory of polarized neutron scattering at grazing incidence is presented. Equations for reflection and scattering cross section are derived in invariant vector form independent of a particular coordinate system and valid for an arbitrary orientation between the incident polarization vector and the direction of the polarization analysis. This provides a solid theoretical background for implementation of 3-dimensional (vector, spherical) polarization analysis into reflectometry. Super-Matrix (SM) and Spin-Recursive (SR) routines are introduced in an easy-to-program form. They allow to create fast–converging and stable numerical algorithms for simulations of spin-flip and non-spin-flip reflectivity profiles for layered systems with magnetization arrangement of arbitrary complexity.

9.1 Introduction

In the extended Introduction I firstly discuss some general questions, related to the symmetry, conservation laws, procedure of averaging, approximations, etc., which are often not well addressed in the text books, but very important for the qualitative interpretation of experimental data on polarized neutron reflection and scattering at grazing incidence. Precise definitions then will be introduced in the main body of the Lecture, where explicit derivations of equations used in numerical simulations for quantitative analysis of experimental data are presented. The theory of polarized neutron scattering in solids and its applications to various problems of magnetism has already received an exhaustive coverage in three Lectures by Maleyev [1] (see this volume). However, the general equations derived and comprehensively

analyzed in Ref.1 are not fully appropriate for polarized neutron reflection and off–specular scattering from magnetic layered systems. This is mostly due to the fact, that it was implicitly assumed that magnetic scattering is relatively week and the Born Approximation (BA) i.e the first order of the perturbation approach, is well applied [2]. In the present Lecture we shall concentrate on a circle of problems related to reflection and scattering of polarized neutrons from magnetic systems, the case when the Born approximation mostly fails. The equations derived below generalize those given in the Maleyev's Lectures, while apparently collapse to the BA particular case, if the scattering is weak. The other problem not well covered in Ref.1 is the role of coherency of neutron radiation, which is also of great importance for the correct interpretation of data on the polarized neutron reflectometry, and will gain some attention below.

The most spectacular manifestation of the BA failure is the phenomenon of the total external reflection which occurs at the glancing angles of incidence α_i below some critical value α_c. Then almost all intensity incident onto a surface is specularly reflected (scattered). The critical angle α_c of magnetic materials depends on the reflecting material, i.e. its scattering length density (SLD) nb, on the neutron wavelength λ, and on the spin state of neutrons. The dependency of the total reflection on the spin states, as mentioned in Ref.1, is commonly used to polarize neutrons: one of the spin components is totally reflected, while the other one is transmitted and the incident beam is split into two in the reciprocal space. The other way to obtain polarization is to let neutrons through a high field gradient, in which the Stern-Gerlach effect splits the beam in the direct space accordingly to neutron spin states[3]. These two essentially different methods are intimately related: a sharp interface between vacuum and laterally magnetized material provides an almost infinite gradient of magnetic field along the normal to the surface.

Having in mind the reflectivity from a magnetic sample with a flat surface, let us make some general remarks on the behavior of a particle with magnetic moment $\boldsymbol{\mu}$ in the magnetic field $\mathbf{B}(\mathbf{r}) = \mathbf{B}(z)$, assuming for simplicity, that it does not change direction, while its strength depends on the only coordinate z. Let us also assume that $\mathbf{B}(z) = 0$ at $z = \pm\infty$, where particles can freely propagate before, at $z = -\infty$, and after, at $z = \infty$, their interaction with the field. If the classical magnetic moment of the particle is not parallel to B, but tilted at an angle γ, then the vector $\boldsymbol{\mu}$ undergoes Larmor precession (LP). The incident beam containing many particles is polarized, if $\langle\boldsymbol{\mu}\rangle \neq 0$. Then, as explained in the Lecture

by Maleyev[1], neutron polarization $\mathbf{P} \propto \langle \boldsymbol{\mu} \rangle \neq 0$ also experiences LP, a purely classical phenomenon describing the evolution of the classical polarization vector $\mathbf{P}$ in a magnetic field, irrespective to the classical or quantum nature of the magnetic moments. It was also explained, that field inhomogeneities scatter neutrons away of the primary beam cause depolarization. In the alternative approach depolarization is caused by the mixing of the LP phases of neutrons passing via different classical trajectories through a field inhomogeneous in space.

In Maleyev's Lecture[1] the effect of reflection from a magnetic potential was totally ignored. One reason is that the neutron kinetic energy E_k is usually much greater than its potential energy $V(z) = \boldsymbol{\mu}\mathbf{B}(z)$. Due to the same reason in the classical approach deviations of neutrons from their initial direction, and in particular, reflection are also ignored. This is not the case not only for ultracold neutrons, but also if the thermal neutrons propagate at an angle close to $\pi/2$ with respect to the $z-$axis. Then in the field depending only on $z-$coordinates the kinetic energy is decomposed into a sum $E_k = E_\perp + E_\parallel$ with $E_\parallel$ corresponding to the neutron propagation parallel to the plane orthogonal to the $z-$axis. The field does not affect $E_\parallel$ and it is one of the integrals of motion, i.e. a conserved quantity. The other integral of motion is the total energy $E = E_k(z)+V(z) = E_k(-\infty)$. So, inside the field range $E_\perp(z)$ depends on z in a manner providing conservation of the sum $E_\perp(z)+V(z) = E-E_\parallel = \text{const}$. This determines the classical trajectory of the particle. The trajectory within the field range can be quite complicated but kinematics allows finally either transmission through the potential in the initial direction at $z \to \infty$, or specular reflection at $z \to -\infty$. This is just a consequence of the general symmetry and the initial condition, which dictate, that both $E_\parallel$ and $E_\perp$ are the same at $z = \pm\infty$ in the initial and final states.

In the classical limit reflection is possible, if at some point (the point of return) $E_\perp(z_c) = 0$. This equation contains the angle γ between $\boldsymbol{\mu}$ and $\mathbf{B}$ as a parameter and it may have no solution if γ is greater than a certain value. Then particles are transmitted, while the perpendicular component of their magnetic moment receives a precession phase leaving the field range. At $\gamma = \pm\pi/2$ the classical particle does not, obviously, change its trajectory, but only the direction of its magnetic moment. In the opposite case $\gamma = 0, \pi$ no precession is possible, but the particle, in principle, can be reflected and/or transmitted. If $\gamma \neq \pm\pi/2, 0$, and the equation $E_\perp(z) = 0$ has a solution, then the particle is reflected and its magnetic moment gains an additional Larmor precession phase travelling out of the

field range, which compensates the phase gained on the way to the point of return. Thus, depending on the angle γ particles can be either reflected from, or transmitted through the classical potential and this allows to partially polarize an initially unpolarized beam. If an unpolarized monochromatic beam contains an equal amount of particles with magnetic moments parallel, or antiparallel to the field, then either both reflected and transmitted beams are perfectly polarized, or there exists only unpolarized transmitted beam. This is, in particular, true for the rectangular reflection potential, i.e. if $V(z) = V_0$ at $0 \leq z \leq z_0$ and $V = 0$, otherwise. The fact of the total reflection and perfect polarization for such a potential also follows from the quantum mechanical consideration at $z_0 \to \infty$. For the first sight this looks surprising, because the classical approach should fail to deal with a discontinuous variation of the potential and can match the quantum mechanical result for a potential slowly varying over the range of the de Broglie wavelength (its projection onto the z-axis) of the particle [4]. An occasional coincidence of the results just demonstrates the power of symmetry arguments valid in both cases. However, the difference becomes immediately clear if one goes beyond the critical angles, accounting finite z_0, or considering a depolarized beam with distributions of classical magnetic moments different of what is assumed above. Recall, that for spin–1/2 particles the latter has no sense at all.

Everywhere below we shall strictly follow the quantum mechanical consideration, recollecting to the classical analogues, if ever they may serve for the illustration of results and always keeping in mind that measurable quantities, i.e. cross sections, polarization components, etc, are classical objects, mean values obtained after proper averaging over a number of events. From the quantum mechanical point of view an interaction of the spin 1/2 with an optically active media, e.g. magnetic field, results in the Zeeman effect which splits the neutron spectrum into the two branches according to two neutron states with spin projections along with, or opposite to the field direction. As soon as the neutron cannot transfer any energy to the static "infinitely heavy" field different spin components of the neutron wave have different wave vectors and propagate inside the field with different phase velocities. We again assume that the field $\mathbf{B}(z)$ depends upon the only coordinate z considering arbitrary (allowed by the Maxwell electrostatics) profile. It can be approximated by a sequence of step-like functions dividing the z-axis into sufficiently small intervals, in which the field variation is negligible.

Impinging onto a flat border between vacuum and a magnetic medium at a certain angle

the neutron wave cannot transfer the component of the wave vector parallel to the surface. Therefore, the Zeeman effect, the conservation of energy and the lateral projection of the wave vector lead to the neutron wave birefringence: it splits into two components with different wave vector projections onto the normal to the surface. The wave reflected from the surface is, apparently, not split neither in the direct, nor in the reciprocal space and for the both spin components the angle of reflection α_f is equal to the angle of incidence α_i. However, due to the different refractive indexes the reflection amplitudes are different for spin component parallel, or antiparallel to the magnetization vector. In particular, if one of the components of the primarily unpolarized beam is almost totally reflected from, while the other one is well transmitted into the matter, then the reflected neutron beam is nearly perfectly polarized along, while the transmitted beam polarized opposite to the magnetization (or visa versa). Alternatively, the reflected beam remains unpolarized, if the angle of incidence is below the total reflection thresholds for both spin components. Reflected and transmitted beams are partially polarized, in the opposite case of incident angles greater than the angles of the total reflection.

As we shall see, the above statements hold for layered systems with any non-collinear magnetization arrangement. The only nontrivial problem is to determine critical edges for each spin components and the direction along which reflected and transmitted polarizations are directed. For complex system this can be done numerically using the Super-matrix, or Super-iterative procedure generalizing the conventional matrix[5] routine for the case of spin-1/2 reflectances[6] and transmittances from magnetic multilayers. Below we also indicate how to generalize[7] the Parratt formalism[8], an iterative procedure also commonly used for the same purpose. The latter is appeared to be more stable at large thicknesses, or/and large number of layers.

All the coherent phenomena mentioned, e.g. reflection, refraction, birefringence and transmission imply an infinitely extended flat surface. In fact, it means that the lateral projection $l_\parallel$ of the coherence length l_c of the neutron radiation is much smaller than the sample surface. The coherence length l_c is related to the uncertainty δq in the determination of the wave vector transfer q, i.e. a resolution of the instrument comprising the uncertainty $\delta\alpha_i$ in the angle of incidence, azimuthal angular divergency $\delta\chi_i$ of the primary beam, detector angular resolution $\delta\alpha_f$ and $\delta\chi_f$, as well as a degree of monochromatization $\delta\lambda/\lambda$. It is easy to see, that at shallow incidence the uncertainty δq in the momentum transfer $\delta\mathbf{q}$

is quite anisotropic. Thus, in the transverse component $q_\perp \approx (2\pi/\lambda)(\sin\alpha_i + \sin\alpha_f)$ it can roughly be estimated as $\delta q_\perp \sim (2\pi/\lambda)\sqrt{(\delta\alpha_i)^2 + (\delta\alpha_f)^2 + (\alpha_i + \alpha_f)^2(\delta\lambda/\lambda)^2}$ and the transverse coherence length $l_\perp \sim 2\pi/\delta q_\perp$ can reach a value up to a few tenths of a micron. Neutron waves scattered from subjects disposed in the transverse direction at distances smaller than $l_\perp$ still interfere. This interference from scattering from the atomic size scale results in the fact, that one can safely use the continuous media, or the optical potential, approximation until the reciproc of the momentum transfer matches the scale comparable with interatomic distances. In particular, considering polarized neutron scattering at low incidence one can account the interaction of the neutron magnetic moment $\hat{\boldsymbol{\mu}}$ with vector of magnetic induction B, while at high momentum transfer the microscopic Hamiltonian of the magnetic interaction is to be used (see Lecture of Maleyev[1]).

Usually reflectometry uses a slit-like collimation and a resolution in the direction across the reflection plane, i.e. in angles χ_i and χ_f, is relaxed. Then the corresponding uncertainty $\delta q_\chi \sim (2\pi/\lambda)\sqrt{(\delta\chi_i)^2 + (\delta\chi_f)^2}$ in the compoment $q_\chi \approx (2\pi/\lambda)(\sin\chi_i - \sin\chi_f)$ does not allow to resolve at $q_\chi = 0$ objects with an extension greater than $l_\chi \sim 2\pi/\delta q_\chi$, which is usually in the order of dozens of Ångstrøms. If at low incidence onto a magnetic crystal, $q_\chi \neq 0$ and matches to one of the reciprocal lattice vector $\hat{\boldsymbol{\tau}}$, then one can observe so called evanescent wave birefrigent diffraction[9] (see below).

A lateral projection of the coherence length l_α within the reflection plane is, in contrast to l_χ, rather huge and can range from a micron up to sub-millimeter scale[10]. Indeed, the corresponding projection $q_\alpha \approx (2\pi/\lambda)(\cos\alpha_f - \cos\alpha_i) \approx q_\perp(\alpha_i - \alpha_f)/2 \ll q_\perp$ of the lateral momentum transfer is rather small and defined with an accuracy estimated as $\delta q_\alpha \sim (2\pi/\lambda)\sqrt{(\alpha_i\delta\alpha_i)^2 + (\alpha_f\delta\alpha_f)^2}$.

If within the coherence length projections l_χ and l_α the surface can be considered as homogeneously flat, then no lateral momentum can be transferred with an accuracy of the corresponding resolution constrains: δq_χ and δd_α. With this accuracy $\mathbf{q}_\alpha = 0$, $\chi_i = \chi_f$ and $\alpha_i = \pm\alpha_f$. It is important to stress that the conditions for the specular reflection $\chi_i = \chi_f$ and $\alpha_i = \alpha_f$ directly follow from the energy and lateral momentum transfer conservation laws, i.e. they are just a consequences of the symmetry, and obviously independent of the spin states of the incoming and outgoing beams. Therefore, "off-specular reflection", either spin-flip, or non-spin-flip is kinematically forbidden, unless the invariance of the surface with respect to the shift parallel to itself is violated. One of the most common examples of a symmetry

violation is an interfacial roughness[11], which violates the lateral translational invariance and gives rise to off–specular diffuse scattering. The other is a set of magnetic domains[12], which may cause spin–flip and non–spin–flip diffuse scattering, whenever the domain size is smaller than the lateral coherence length. In fact one can still use a term "off-specular reflection", which would mean a coherent Bragg scattering from laterally periodically patterned samples[13], or grazing incidence diffraction[9, 6] by a crystalline structure, which also violates the conservation of the lateral projection of the momentum. All those phenomena are presently well understood and routinely used to investigate magnetic properties of magnetic thin films and multilayers[14].

A separate, almost not investigated case is if both the energy and momentum conservation law are violated. Then not only a portion of the lateral momentum, but also energy is transferred to or received from the sample, creating or absorbing thermal excitations in the film. An observation of a transition between the Zeeman levels split in the ambient field applied perpendicular to the thin ferromagnetic film surface was reported[15] as a manifestation of inelastic off-specular scattering. One, however, should admit that in this configuration the magnetic field is rather inhomogeneous, especially at the sample edges. As soon as the external field $\mathbf{B}(\boldsymbol{\rho})$ depends upon the lateral coordinate $\boldsymbol{\rho}$, the lateral translation invariance is also violated and only the energy conservation law is to be obeyed. The problem becomes 3-dimensional and can be solved only asymptotically, and/or in a few degenerated cases. In one of them $\mathbf{B}(x)$ depends on one lateral coordinate x and essentially varies only far away of the reflection area, being well homogeneous in the immediate vicinity of the surface. Within this range the lateral projection of the neutron momentum is conserved, while the normal component experiences a Zeeman splitting in the ambient, as well as in the internal field of the film. If these fields are not collinear, then both spin states are in general partially populated, and "off-specular spin flip reflection" does not require any energy exchange with the sample. Within the range of reflection (coherence length) both the total energy and the lateral projection of the momentum are conserved, while propagating to the border of the field, both beams are deflected, and after exiting the range of the field, different spin components have lateral and transverse wave vectors such that each of the components has the same energy as in the incident beam before the interaction with the compound field+sample.

This is, in fact, one of the so-called finite size effects. The other are other almost trivial

effects of that sort. One of them consists in the splitting of the beam refracted from a side edge of a relatively thick magnetized slab after the incidence onto its surface. Another one is the splitting at reflection, if the beam is incident through the edge of a magnetized sample, while the reflected beams exit through its opposite side edge. The latter example, actually, reproduces a kinematics discussed above if one adds on top of the thick slab a film magnetized non-collinearly with the slab. A further example of the sample size effect is the thin-film neutron waveguiding[16], where the scattering signal is observed not only at the angles of specular reflection, but also in the direction along the sample surface.

Here we shall not discuss these scope of questions in more details and after this long Introduction, we turn to the derivation of equations for polarized neutron scattering cross sections. In the next section we shall introduce some definitions, and remind relevant chapters from the textbooks on Quantum Mechanics[4].

9.2 Spin states and polarization vector

In this Section we remind how starting from quantum spin states of a spin–1/2 particle to arrive at the classical polarization vector of the beam consisting of those particles. As well known, the particle behavior in this case is formally described by the two component vector of the states:

$$|\Psi(\mathbf{r})\rangle = \Psi^{+}(\mathbf{r})|\chi^{+}\rangle + \Psi^{-}(\mathbf{r})|\chi^{-}\rangle = \begin{pmatrix} \Psi^{+} \\ \Psi^{-} \end{pmatrix}, \tag{1}$$

i.e. by a pair of complex functions $\Psi^{\pm}(\mathbf{r}) = |\Psi^{\pm}|\exp(\mathrm{i}\phi_{\pm})$, which are the "+" and "-" projections onto two-component basic vectors

$$|\chi^{+}\rangle = \begin{pmatrix} 1 \\ 0 \end{pmatrix} \quad \text{and} \quad |\chi^{-}\rangle = \begin{pmatrix} 0 \\ 1 \end{pmatrix}. \tag{2}$$

These vectors being orthogonal and properly normalized:

$$\langle\chi^{+}|\chi^{-}\rangle = \langle\chi^{-}|\chi^{+}\rangle = 0, \quad \langle\chi^{+}|\chi^{+}\rangle = \langle\chi^{-}|\chi^{-}\rangle = 1, \tag{3}$$

complete a basis in the discrete 2-D space of spin states and the projections $\Psi^{\pm}(\mathbf{r})$ have the sense of the probability amplitudes to find the particle in one the states labelled as "+" , or "-". The four functions: the amplitudes $\Psi^{\pm}$ and the phases $\chi^{\pm}$ depend on the choice of the quantization axis, while the probability to find the particle in any of those states is a scalar product $\langle\Psi|\Psi\rangle = \sum_{\alpha}|\Psi^{\alpha}|^2$, i.e. the only invariant independent of the coordinate system.

If particles are "produced" by a source, then a measurable quantity, such as the particles density (or flux) is found via averaging $\langle\Psi|\Psi\rangle$ over the counting time of particles. For a stationary source this averaging is usually substituted by averaging over statistics of the source states. Then the particle number density,

$$\rho_0 = \overline{\langle\Psi|\Psi\rangle}^{\,\text{source}} = \overline{|\Psi^+|^2 + |\Psi^-|^2}^{\,\text{source}} = \text{Tr}\overline{\{|\Psi\rangle\langle\Psi|\}}^{\,\text{source}} = \text{Tr}\hat{\rho}, \tag{4}$$

is expressed via the sum of the diagonal elements of the density matrix

$$\hat{\rho} = \overline{|\Psi\rangle\langle\Psi|}^{\,\text{source}} = \begin{pmatrix} \rho^{++} & \rho^{+-} \\ \rho^{-+} & \rho^{--} \end{pmatrix}. \tag{5}$$

where $\rho^{\mu\nu} = \overline{\Psi^\mu \Psi^{\nu *}}^{\,\text{source}}$, with $\mu, \nu = +, -$.

Four real elements of the density matrix complete a full set of quantities accessible for an observation, instead of four initial quantities: two amplitude modula $|\Psi^\pm|$ and two phases $\chi^\pm$, characterizing quantum spin states. In contrast to the latter ones, the density matrix incorporates also an information on the statistical properties of the source. However, it is still inconvenient that the matrix elements explicitly depend on the particular choice of the representation, determined by the quantization axis, or in other words, on the choice of the coordinate system.

In order to avoid this inconvenience, the elements of the matrix in Eq.(5) should be classified is a particular manner using the fact that any 2×2 matrix $\rho^{\mu\nu}$ can be decomposed over four matrices as follows:

$$\begin{pmatrix} \rho^{++} & \rho^{+-} \\ \rho^{-+} & \rho^{--} \end{pmatrix} = \frac{\rho_0}{2}\left\{ \begin{pmatrix} 1 & 0 \\ 0 & 1 \end{pmatrix} + P_x \begin{pmatrix} 0 & 1 \\ 1 & 0 \end{pmatrix} + P_y \begin{pmatrix} 0 & -i \\ i & 0 \end{pmatrix} + P_z \begin{pmatrix} 1 & 0 \\ 0 & -1 \end{pmatrix} \right\}, \tag{6}$$

where four real quantities ρ_0,

$$P_x = \{\rho^{+-} + \rho^{-+}\}/\rho_0 \tag{7}$$

$$P_y = \text{i}\{\rho^{+-} - \rho^{-+}\} = /\rho_0 \tag{8}$$

$$P_z = \{\rho^{++} - \rho^{--}\}/\rho_0 \tag{9}$$

serve for an alternative parametrization of the matrix $\rho^{\mu\nu}$.

This parametrization is rather convenient, because the four matrices in the right hand side of Eq.(6) are just the unit matrix $\hat{I}$ and three Pauli matrices σ_x, σ_y, and σ_z:

$$\hat{I} = \begin{pmatrix} 1 & 0 \\ 0 & 1 \end{pmatrix};\ \hat{\sigma}_x = \begin{pmatrix} 0 & 1 \\ 1 & 0 \end{pmatrix};\ \hat{\sigma}_y = \begin{pmatrix} 0 & -i \\ i & 0 \end{pmatrix};\ \hat{\sigma}_z = \begin{pmatrix} 1 & 0 \\ 0 & -1 \end{pmatrix}. \tag{10}$$

These matrices are mutually orthogonal: $\hat{\sigma}_\alpha\hat{\sigma}_\beta = 0$ at $\alpha \neq \beta$, while $\hat{\sigma}_\alpha\hat{\sigma}\beta = 1$ at $\alpha = \beta$, i.e.

$$\sigma_\alpha\sigma_\beta \;\; = \;\; \delta_{\alpha\beta} + \mathrm{i}\varepsilon_{\alpha\beta\gamma}\sigma_\gamma, \tag{11}$$

where $\{\alpha, \beta, \gamma\} = \{x, y, z\}$, and $\delta_{\alpha\beta}$ is the Kronecker symbol: $\delta_{\alpha=\beta} = 1$, $\delta_{\alpha\neq\beta} = 0$, $\varepsilon_{\alpha\beta\gamma} = -\varepsilon_{\beta\alpha\gamma} = -\varepsilon_{\alpha\gamma\beta}$ is the Levi-Civita tensor, i.e. totally antisymmetric axial tensor of third rank: $\varepsilon_{\alpha\neq\beta\neq\gamma} = \pm 1$, while $\varepsilon_{\alpha\beta\gamma} = 0$, otherwise.

Due to these properties the three matrices σ_α can be considered as projections of 3D pseudo-vector $\hat{\boldsymbol{\sigma}}$ onto the Cartesian basis, and Eq.(6) is written in an invariant vector form, independent of the choice of the coordinate system:

$$\hat{\rho} = \frac{\rho_0}{2}\{\hat{I} + P_x\hat{\sigma}_x + P_y\hat{\sigma}_y + P_z\hat{\sigma}_z\} = \frac{\rho_0}{2}\{\hat{I} + (\mathbf{P}\hat{\boldsymbol{\sigma}})\}, \tag{12}$$

The axial vector $\mathbf{P}$ is called the polarization vector of the density matrix. It is determined as:

$$\mathbf{P} = \overline{\langle\Psi|\hat{\boldsymbol{\sigma}}|\Psi\rangle}^{\,\mathrm{source}} = \mathrm{Tr}\{\hat{\rho}\hat{\boldsymbol{\sigma}}\}/\mathrm{Tr}\hat{\rho}, \tag{13}$$

i.e. as an expectation value of the vector $\hat{\boldsymbol{\sigma}}$.

In a particular coordinate system, due to Eqs.(7–9):

$$P_x \;\; = \;\; 2\{\overline{|\Psi^+||\Psi^-|\cos\phi}\}/\{\overline{|\Psi^+|^2 + |\Psi^-|^2}\} \tag{14}$$

$$P_y \;\; = \;\; -2\{\overline{|\Psi^+||\Psi^-|\sin\phi}\}/\{\overline{|\Psi^+|^2 + |\Psi^-|^2}\} \tag{15}$$

$$P_z \;\; = \;\; \{\overline{|\Psi^+|^2} - \overline{|\Psi^-|^2}\}/\{\overline{|\Psi^+|^2 + |\Psi^-|^2}\}, \tag{16}$$

where $\phi = \phi^+ - \phi^-$ is a phase shift. If it is absolutely random and varies uncontrollably for different particles, then $\overline{\cos\phi} = \overline{\sin\phi} = 0$, $P_x = P_y = 0$ and the matriz $\hat{\rho}$ is diagonal. If at the same time $\rho^{++} \neq \rho^{--}$, then $P_z \neq 0$ and the density matrix has a polarization along $z-$axis. In the opposite case $P_z = 0$, but $P_x \neq 0$ and $P_y \neq 0$, the polarization is displayed in the basic plane and their projections can be either correlated, or not. If at perfect phase correlation $\overline{\cos\phi} = 1$, then $\overline{\sin\phi} = 0$ and visa versa. From Eqs.(14-16) it immediatelly follows, that in general, $|\mathbf{P}| \leq 1$.

In a neutron scattering experiment one measures not density, but rather neutron flux, defined as

$$\mathbf{j} = \frac{\mathrm{i}\hbar}{2m}\lim_{\mathbf{r}\to\mathbf{r}'}\{\nabla_{\mathbf{r}} - \nabla_{\mathbf{r}'}\}\overline{\langle\Psi(\mathbf{r})\Psi(\mathbf{r}')\rangle}. \tag{17}$$

The corresponding extension of the consideration above for this quantity is just obvious.

9.3 Evolution of Density Matrix and Polarization Vector

In this section we consider, again formally, the evolution of the components of the density matrix and of the polarization vector under the action of some generalized (pseudo–) vector field, which can be magnetic, pseudo–nuclear, or any other, just having a proper symmetry with respect to space and time parity[1].

An initial 2D vector of spin 1/2 states $|\Psi_{i0}\rangle$ is developed into another 2D vector of states $|\Psi_i\rangle = \hat{\mathcal{S}}_i|\Psi_{i0}\rangle$ by some 2×2 $\hat{\mathcal{S}}_i-$matrix. As any 2×2 matrix, the latter can generally be parametrized in the same way as the density matrix in Eqs.(12,13):

$$\hat{\mathcal{S}}_i(\hat{\boldsymbol{\sigma}}) = \hat{1}\mathcal{S}_i + (\boldsymbol{\mathcal{S}}_i\hat{\boldsymbol{\sigma}}) \tag{18}$$

$$\mathcal{S}_i = \frac{1}{2}\mathrm{Tr}\{\hat{\mathcal{S}}_{\mathrm{i}}\} \quad ; \quad \boldsymbol{\mathcal{S}}_i = \frac{1}{2}\mathrm{Tr}\{\hat{\mathcal{S}}_{\mathrm{i}}\hat{\boldsymbol{\sigma}}\}, \tag{19}$$

i.e. via four complex functions: one scalar, $\mathcal{S}_i$, and three components of the vector, $\boldsymbol{\mathcal{S}}_i$.

The expectation value $\overline{\langle\Psi_i|\Psi_i\rangle} = \mathrm{Tr}\overline{|\Psi_{\mathrm{i}}\rangle\langle\Psi_{\mathrm{i}}|} = \mathrm{Tr}\hat{\rho}_{\mathrm{i}}$, is written via the density matrix:

$$\hat{\rho}_i = \hat{\mathcal{S}}_i\hat{\rho}_{i0}\hat{\mathcal{S}}_i^{+} = \{\mathcal{S}_i + (\boldsymbol{\mathcal{S}}_i\hat{\boldsymbol{\sigma}})\}\{1 + (\boldsymbol{P}_{0i}\hat{\boldsymbol{\sigma}})\}\{\mathcal{S}_i^{*} + (\boldsymbol{\mathcal{S}}_i^{*}\hat{\boldsymbol{\sigma}})\} \tag{20}$$

"developed" out of the initial density matrix

$$\hat{\rho}_{i0} = \{\rho_{i0} + (\boldsymbol{\mathcal{P}}_{i0}\hat{\boldsymbol{\sigma}})\} = \rho_{i0}\{1 + (\boldsymbol{P}_{i0}\hat{\boldsymbol{\sigma}})\}, \tag{21}$$

by the $\hat{\mathcal{S}}_i-$matrix. Substitution of Eq.(18,19) into Eq.(20) and use of Eq.(11) results in the following equation for the "developed" density matrix:

$$\hat{\rho}_i = \{\rho_i + (\boldsymbol{\mathcal{P}}_i\hat{\boldsymbol{\sigma}})\} = \rho_i\{1 + (\boldsymbol{P}_i\hat{\boldsymbol{\sigma}})\}, \tag{22}$$

where $\boldsymbol{P}_i = \boldsymbol{\mathcal{P}}_i/\rho_i$ is the modified polarization, $\rho_i = \frac{1}{2}\mathrm{Tr}\{\hat{\rho}_{\mathrm{i}}\}$, $\boldsymbol{\mathcal{P}}_i = \frac{1}{2}\mathrm{Tr}\{\hat{\rho}_{\mathrm{i}}\hat{\boldsymbol{\sigma}}\}$, and so:

$$\rho_i = \{|\mathcal{S}_i|^2 + |\boldsymbol{\mathcal{S}}_i|^2\} + 2\Re\{\mathcal{S}_i(\boldsymbol{\mathcal{S}}_i^{*}\boldsymbol{P}_{0i})\} + \Im\{([\boldsymbol{\mathcal{S}}_i\times\boldsymbol{\mathcal{S}}_i^{*}]\boldsymbol{P}_{0i})\}, \tag{23}$$

$$\boldsymbol{\mathcal{P}}_i = \{|\mathcal{S}_i|^2 - |\boldsymbol{\mathcal{S}}_i|^2\}\boldsymbol{P}_{0i} + 2\Re\{\boldsymbol{\mathcal{S}}_i[\mathcal{S}_i^{*} + (\boldsymbol{\mathcal{S}}_i^{*}\boldsymbol{P}_{0i})]\} + \Im\{[\boldsymbol{\mathcal{S}}_i\times\boldsymbol{\mathcal{S}}_i^{*}]\} + 2(\mathcal{S}_i[\boldsymbol{\mathcal{S}}_i^{*}\times\boldsymbol{P}_{0i}]) \tag{24}$$

At first sight these equations look quite complicated, but they are well structured and transparent from the symmetry point of view. Indeed, the first term in Eq.(23) is independent of the incident polarization $\mathbf{P}_{0i}$, while the two others are proportional to different components of $\mathbf{P}_{0i}$: the second one to the projection of $\mathbf{P}_{0i}$ onto the direction of $\boldsymbol{\mathcal{S}}_i$, whereas the last is only not equal to zero, if $\mathbf{P}_{0i}$ has component perpendicular to $\boldsymbol{\mathcal{S}}_i$ and $\boldsymbol{\mathcal{S}}_i^{*}$. This term vanishes if the vector $\boldsymbol{\mathcal{S}}_i$ has only real components, and in particular, in the Born approximation.

In accordance to Eq.(24), the polarization vector is generally composed of three vectors. Two of them are directed either along with, or perpendicular to the incident polarization vector $\mathbf{P}_{0i}$. The direction of the third one is independent of $\mathbf{P}_{0i}$ having components either parallel and perpendicular to the vector $\boldsymbol{\mathcal{S}}_i$. Again, the two last terms in Eq.(24) vanish in the BA. A simplest example where one can easily go beyond of BA, is the Larmor precession in a magnetic field considered in the next Section.

9.4 Larmor Precession

The equation for Larmor precession was derived and thoroughly analyzed in Maleyev's Lecture[1]. Nonetheless in this Section I shall do it once again giving an exercise which shows how the LP immediately follows from the Schrödinger examining the approximations on the way. Let us assume that a polarized beam falls onto a sample having a form of a slab magnetized along one of its long faces. For the sake of simplicity let us first neglect the neutron interaction with nuclei, which is not important for the derivation of LP. Then in the Schrödinger equation

$$\{\hat{1}(\hbar^2/2m)[\nabla^2 + k_0^2] - \hat{V}(\mathbf{r})\}|\Psi(\mathbf{r})\rangle = 0, \tag{25}$$

the operator $\hat{V}(\mathbf{r}) = \hat{\boldsymbol{\mu}}\mathbf{B}(\mathbf{r})$ describes the magnetic interaction of the neutron magnetic moment μ, with the magnetic field inductance $\mathbf{B}(\mathbf{r})$, $\hat{\boldsymbol{\mu}} = \mu\hat{\boldsymbol{\sigma}}$ is proportional to the vector of the Pauli matrices $\hat{\boldsymbol{\sigma}}$, $k_0 = 2\pi/\lambda$ is the incoming neutron wave number.

The solution of this equation is formally given as: $|\Psi(\mathbf{r})\rangle = \hat{\mathcal{S}}(\mathbf{r})|\Psi_0\rangle$, via the 2×2 $\hat{\mathcal{S}}-$matrix and the initial vector of states $|\Psi_0\rangle$ is defined at a distance away from the sample, where $\mathbf{B} = 0$. We assume, that $|\Psi_0\rangle = \mathrm{e}^{i\mathbf{k}_0\mathbf{r}}|\psi_0\rangle$, where $\mathbf{k}_0$ is the incoming wave vector.

If the field $\mathbf{B}(\mathbf{r}) = \mathbf{B}$ inside the slab is homogeneous, then the matrices $\hat{V}$ and, correspondingly, $\hat{\mathcal{S}}(\mathbf{r})$ are diagonal at the quantization axis directed along the unit vector $\mathbf{b} = \mathbf{B}/|\mathbf{B}|$ and the matrix $\hat{\mathcal{S}}(\mathbf{r})$ has only two non–zero elements $\mathcal{S}^+(\mathbf{r})$ and $\mathcal{S}^-(\mathbf{r})$. Due to the slab geometry $\mathcal{S}^\pm = \mathcal{S}^\pm(z)\mathrm{e}^{\mathrm{i}\boldsymbol{\kappa}\boldsymbol{\rho}}$, where $\boldsymbol{\kappa}$ is the lateral projection of the wave vector, $\boldsymbol{\rho}$ is in-plane, while z is the normal to the slab face coordinate, and

$$\mathcal{S}^\pm(z) = \mathrm{e}^{i\varphi_\pm(z)}t_\pm + \mathrm{e}^{-i\varphi_\pm(z)}r_\pm. \tag{26}$$

Here $\varphi_\pm = p_\pm z$ are the phase shifts for the neutron wave spin components with positive, or negative spin projection onto the field direction, $p_\pm = \sqrt{p_0^2 - p_{c\pm}^2}$ are normal to the surface components of the wave vector inside the slab, $p_0 = k_0 \sin\alpha$ is the normal projection of the

wave vector incoming at the glancing angle α (let us assume no field outside the slab), and $\hbar^2 p_{c\pm}^2/2m = \mu B$. In Eq.(26) the first term corresponds to waves transmitted into the slab through its front face with the amplitudes $t_\pm$, while the second one describes the propagation of the wave reflected from its back face with the amplitudes $r_\pm$. Those amplitudes will be found in the next Section, but here we just emphasize that both transmitted and reflected waves are split into two components in accordance to the spin projections and each of those components propagate with different phase velocities and interfere with each other within the coherence length. This interference in certain approximations results, as we shall see, in LP. To show this, let us suppose that the angle of incidence α is not very small and such that $p_0 \gg p_{c\pm}$. Then, the reflection effect is weak and in a first approximation can be just neglected, whereas $t_\pm \approx 1$ and

$$\mathcal{S}^\pm(z) \approx \mathrm{e}^{i\varphi_\pm(z)}. \tag{27}$$

It is easy to check, that $\mathcal{S}^\pm$ are the eigenvalues of the matrix

$$\hat{\mathcal{S}}(z) = \mathrm{e}^{i\hat{\varphi}(z)} = \frac{1}{2}\{\hat{1}(\mathrm{e}^{i\varphi^+} + \mathrm{e}^{i\varphi^-}) + (\hat{\boldsymbol{\sigma}}\mathbf{b})(\mathrm{e}^{i\varphi^+} - \mathrm{e}^{i\varphi^-})\}. \tag{28}$$

Indeed, $(\hat{\boldsymbol{\sigma}}\mathbf{b}) = b_x\hat{\sigma}_x + b_y\hat{\sigma}_y + b_z\hat{\sigma}_z$, and if z-axis is chosen parallel to $\mathbf{b}$, then $b_z = 1$, and $\hat{\mathcal{S}}$ is diagonal with diagonal elements given in Eq.(27). Actually, Eq.(28) is a consequence of a general theorem[4], which sounds as follows: any scalar function $\hat{f} = \hat{f}(\hat{\boldsymbol{\sigma}})$ of the vector $\hat{\boldsymbol{\sigma}}$ of the Pauli matrices is linear with respect to $\hat{\boldsymbol{\sigma}}$:

$$\hat{f} = \hat{1}f + (\hat{\boldsymbol{\sigma}}\mathbf{f}), \tag{29}$$

where $f = \mathrm{Tr}\{\hat{f}\}/2$, and $\mathbf{f} = \mathrm{Tr}\{\hat{f}\hat{\boldsymbol{\sigma}}\}/2$.

The equation for the outgoing polarization vector $\mathbf{P}_f$ can be obtained from Eqs.(13,20), or via an immediate substitution of the equations

$$\mathcal{S} = \frac{1}{2}\{(\mathrm{e}^{i\varphi^+} + \mathrm{e}^{i\varphi^-}\} \text{ and } \boldsymbol{\mathcal{S}} = \frac{\mathbf{b}}{2}\{\mathrm{e}^{i\varphi^+} - \mathrm{e}^{i\varphi^-})\} \tag{30}$$

following from Eq.(28) into Eq.(24). This would not give, however, more complicated equation than that for the Larmor precession derived in Ref.1. It would coincides with the LP equation, only if one approximates $p_\pm \approx p_0 \mp \omega/2v$, where $\omega = \mu B/\hbar$ is the LP frequency and $v = \hbar k_0 \sin\alpha/m$ is a group velocity projection onto normal to the surface. Then, instead of Eqs.(31), one has:

$$\mathcal{S} \approx \mathrm{e}^{ip_0 z}\cos\varphi/2 \text{ and } \boldsymbol{\mathcal{S}} \approx \mathrm{i}\frac{\mathbf{b}}{2}\mathrm{e}^{ip_0 z}\sin\varphi/2, \tag{31}$$

where $\varphi = \omega z/v$ is the LP phase shift at a distance z from the front face of the slab.

In this approximation the polarization vector

$$\mathbf{P} = \mathbf{b}(\mathbf{P}_0\mathbf{b}) + [\mathbf{P}_0 - \mathbf{b}(\mathbf{P}_0\mathbf{b})]\cos\varphi + [\mathbf{b}\times\mathbf{P}_0]\sin\varphi. \tag{32}$$

is expressed via the polarization vector $\mathbf{P}_0$ in the same way, as in Ref.1.

One should, however, admit that not all approximations above are obvious. Thus, for $\mu B \ll E\sin^2\alpha$ and not very small angles α, the reflection can certainly be neglected. On the other hand, a truncation of expansions of the phases $\varphi_\pm$ in the exponents in Eq.(31) is only reasonable at $z \ll \lambda(\mu B/E)^2/\sin^5\alpha$. Otherwise, the LP is distorted by the refraction effects. The consideration above and the LP equation, particularly, accounts for the interference of birefringent wave components. So, distortions of LP can be seen if the coherence length along the $z-$ direction is larger than the scale indicated above. In the opposite case the beam is partially depolarized before these distortions become visible.

If the magnetic field varies along the $z-$direction on a distance smaller than the corresponding projection of the coherence length, then one can divide the slab into N small slices of thickness $d_l = z_l - z_{l-1}$ such, that within each slice numerated by $1 \le l \le N$, i.e. at $z_{l-1} \le z \le z_l$, a field variation can be neglected and approximated as $\mathbf{B}(z) \approx \mathbf{B}_l$. Then

$$\hat{\mathcal{S}}(z) = \prod_l \hat{\mathcal{S}}_l = \prod_l \exp(i\hat{\varphi}_l), \tag{33}$$

where $\hat{\varphi}_l = p_l d_l$ is the phase shift over $d_l = z_l - z_{l-1}$. This equation can be rewritten in an equivalent, but more elegant symbolic form as:

$$\hat{\mathcal{S}}(z) = \hat{\mathrm{T}}_z \int_0^z \mathrm{d}z' \exp(i\hat{\varphi}'(z')), \tag{34}$$

where $\hat{\mathrm{T}}_z$ is a "chronological" operator, and $\hat{\varphi}'(z')$ is the derivative of the phase operator at the point with the coordinate z'. The latter form can be more convenient for some cases of field variations.

At the same circumstances as above the partial $\hat{\mathcal{S}}_l$-matrix is determined by the equation:

$$\hat{\mathcal{S}}_l = \frac{1}{2}\{(\mathrm{e}^{i\varphi_l^+} + \mathrm{e}^{i\varphi_l^-}) + (\boldsymbol{\sigma}\mathbf{b}_l)(\mathrm{e}^{i\varphi_l^+} - \mathrm{e}^{i\varphi_l^-})\} \tag{35}$$

$$\approx \mathrm{e}^{ik_0 d_l}\{\cos(\varphi_l/2) + i(\boldsymbol{\sigma}\mathbf{b}_l)\sin(\varphi_l/2)\}, \tag{36}$$

where $\varphi_l^\pm = p_{l\pm} d_l$, $p_{l\pm} = \sqrt{p_0^2 \mp p_{cl}^2} \approx p_0 \mp (\omega_l/2v)$, $\varphi_l = \omega_l d_l/v$, $\omega_l = \mu B_l/\hbar$ is the Larmor frequency in the slice l, and $\mathbf{B}_l = B_l\mathbf{b}_l$. Consequently, the partial polarization vector in the

slice l,

$$\mathbf{P}_l = \mathbf{b}_l(\mathbf{P}_{l-1}\mathbf{b}_l) + [\mathbf{P}_{l-1} - \mathbf{b}_l(\mathbf{P}_{l-1}\mathbf{b}_l)]\cos\varphi_l + [\mathbf{b}_l \times \mathbf{P}_{l-1}]\sin\varphi_l, \tag{37}$$

is expressed via the polarization vector $\mathbf{P}_{l-1}$ in the previous slice in the same way, as the polarization vector $\mathbf{P}$ is expressed via the vector of incoming polarization $\mathbf{P}_0$ in Eq.(32). It must be pointed out, that Eq.37 is not very useful because partial polarization vectors $\mathbf{P}_l$ are not those quantities experimentally measured. On the other hand, the final polarization vector obeys Eq.(32), even in general case considered above, if the phase φ is substituted by some effective phase of "precession" around some direction in space, instead of that as pointed in Eq.(32) by the unit vector $\mathbf{b}$. For complicated field arrangement this phase and direction are given by four Eqs.(31), as soon as the $\hat{\mathcal{S}}-$matrix is computed using Eq.(34-37).

As mentioned above, the finite coherence length causes depolarization, which is taken into account by convolution of Eq.(32) with the resolution function, including the divergence and the wave–length spread of the primary beam, as well as the finite acceptance aperture of the detector. The latter is important if the field is inhomogeneous within the scale of the lateral projection of the coherence length. Then it may cause scattering beyond the angular range of the primary beam divergence and acceptance aperture of the analyzer. Due to that some intensity and polarization is lost (see, Lecture of Maleyev[1]), while in the consideration above it was silently supposed that all neutrons are safely arrived at the perfect analyzer and detector.

Even though, depolarization may occur if the field is laterally homogeneous over the scale smaller than the corresponding projection of the coherence length, but it varies at greater distances. One of the examples is of large magnetic domains, usually not seen in scattering experiments, but effectively depolarize the beam. Hence, the polarization vector $\mathbf{P}$ should be calculated for each of the direction of domain induction, given in Eq.(32) $\mathbf{b}$, and the result is then to be averaged over all possible directions of $\mathbf{b}$ in accordance with the statistics of the domains (see, for details, Ref.1).

It is important to note, that for large domains one cannot say much about their size and size distribution. However, as it was discussed in the Introduction, the angle of incidence α can play the role of a parameter, controlling the lateral projection of the coherence length, which at low angles may exceed the typical domain size. Next, one should take care about the optical effects, i.e. reflection and refraction, but due to the huge coherence length projection onto the surface plane, one can resolve this size with small angle off-specular scattering.

9.5 Reflectance and Transmittance Matrixes

Continuing the discussion of the previous Section, we shall consider here the interaction of polarized neutrons with a slab–shape magnetized sample in the case of a shallow incidence of the beam at its surface. As it was discussed in the Introduction, under this circumstances one of the projection $l_{\|}$, i.e. that is in the reflection plane, of the beam coherence length l_c onto the sample surface can be rather large.

Therefore, the neutron wave averages out most of the details of the surface structure over a scale $l_{\|}$ and the main portion of the incident beam is either transmitted through, or reflected from the sample without appreciable changes in its lineshape, provided both sample faces are well parallel to each other and macroscopically flat. At the same time, the beam can dramatically change its polarization, as it was shown above for the transmission, while reflection was totally neglected. Here we concentrate mostly on reflection, keeping in mind that, both the transmitted beam intensity and its polarization are drastically affected by the presence of reflection.

Similar to the previous Section we solve the Schrödinger equation Eq.(25) assuming that the interaction potential (operator in the spin space) $\hat{V}(\mathbf{r})$ averaged over the lateral coherence length depends on the only coordinate z, i.e. $\langle\hat{V}(\mathbf{r})\rangle_\rho = \hat{V}(z)$. Let us divide the slab, as above, into slices writing down

$$\hat{V}(z) = \sum_{l=1}^{N}\{\hat{V}_{Nl} + \hat{V}_{Ml}\}, \tag{38}$$

where, $\hat{V}_{Nl} = \hat{1}V_{Nl}$ at $\leq z_{l-1} \leq z \leq z_l$ and V_{Nl} is the nuclear optical potential (if interaction with nuclear spin is neglected) of the l^{th} slice. The magnetic part of the interaction operator $\hat{V}_{Ml} = -\hat{\boldsymbol{\mu}}\mathbf{B}_l$ is defined as above, with the neutron magnetic moment operator $\hat{\boldsymbol{\mu}} = \mu\hat{\boldsymbol{\sigma}}$, $\mu = \gamma\mu_N$, μ_N is nuclear magneton and $\gamma = -1.91$. Note that artificially synthesized layered films are divided into a sequence of layers with relatively sharp interfaces. Therefore, below we shall often use a term "layer" instead of "slice", as well as "film", rather than "slab".

Due to the same symmetry conditions as in the preceding Section, the lateral and transverse variables are separated and the solution of Eq.(25) is factorized into the product, but the asymptotic conditions now also include the reflected wave, and above the surface:

$$|\Psi(\mathbf{r})\rangle = \exp(i\boldsymbol{\kappa}\boldsymbol{\rho})\{e^{ip_0 z} + e^{-ip_0 z}\hat{R}\}|\psi^i(0)\rangle, \tag{39}$$

where $\boldsymbol{\kappa}$ is the in-plane (conserved) projection of wave vector $\mathbf{k}_0$, $p_0 = \sqrt{k_0^2 - \kappa^2}$ is its

component normal to the surface, $\boldsymbol{\rho}$ is the lateral coordinate, $|\psi^i(0)\rangle$ is the initial vector of states at the surface, $\hat{R}$ is the reflectance matrix transforming components of the incoming wave function $|\psi^i(0)\rangle$ into the components of the reflected wave

$$|\psi^f(0)\rangle = \hat{R}|\psi^i(0)\rangle. \tag{40}$$

An explicit expression for the reflectance matrix $\hat{R}$ for a semi–infinite magnetic sample was found, to the best of our knowledge, for the first time by Felcher et al.[17] by writing the interaction matrix in the laboratory coordinate system:

$$\hat{V} = \begin{pmatrix} V_N - \mu B^z & \mu(B^x - iB^y) \\ \mu(B^x + iB^y) & V_N + \mu B^z \end{pmatrix}, \tag{41}$$

solving Eq.(25) in the magnetic medium, and then matching the components of the vector $|\psi(z)\rangle$ and their first derivatives at the surface. Finally, the continuity conditions at the surface were collected into a 4×4 matrix equation of a quite complicated structure, which made it difficult to adjust the method for routine calculations of the reflectivity from multilayered systems.

As we shall see, the boundary conditions at the interfaces can be written in a substantially simplified form, if one keeps the potential in the vector form independent of the coordinate and uses the algebra of the Pauli matrices. To do so one should just notice that the vector of states $|\psi_l(s)\rangle$ inside any layer l can be written via the vector of initial states $|\psi(0)\rangle$ as follows:

$$|\psi_l(z)\rangle = \hat{\mathcal{S}}_l(z, \boldsymbol{\sigma})|\psi_l^i(0)\rangle, \tag{42}$$

where the $\hat{\mathcal{S}}_l$–matrix is written in the form

$$\hat{\mathcal{S}}_l(z, \boldsymbol{\sigma}) = \mathrm{e}^{i\hat{\varphi}_l(z)}\hat{t}_l + \mathrm{e}^{-i\hat{\varphi}_l(z)}\hat{r}_l, \tag{43}$$

which takes into account the neutron waves refracted through and reflected from the interfaces. Here $\hat{\varphi}_l(z) = \hat{p}_l(z - z_{l-1})$, and $z_0 = 0$. The wave vector operator $\hat{p}_l = \sqrt{p_0^2 - \hat{p}_{lc}^2}$ is diagonal at $z \parallel \overline{\mathbf{B}}_l$, with the eigenvalues $p_{l\pm} = \sqrt{p_0^2 - p_{cl\pm}^2}$, $p_{cl\pm}^2 = 4\pi(\overline{nb}_{Nl} \mp \overline{nb}_{Ml})$, $\overline{nb}_{Nl}$ and $\overline{nb}_{Ml}$ are the mean nuclear and magnetic scattering length densities within the l^{th} layer.

The continuity conditions at subsequent interfaces,

$$|\psi_{l+1}(z_{l+1})\rangle = |\psi_l(z_{l+1})\rangle \tag{44}$$

$$|\psi'_{l+1}(z_{l+1})\rangle = |\psi'_l(z_{l+1})\rangle \tag{45}$$

look as follows:

$$\hat{t}_{l+1} + \hat{r}_{l+1} = e^{i\hat{\varphi}_l}\hat{t}_l + e^{-i\hat{\varphi}_l}\hat{r}_l \tag{46}$$

$$\hat{p}_{l+1}\{\hat{t}_{l+1} - \hat{r}_{l+1}\} = \hat{p}_l\{e^{i\hat{\varphi}_l}\hat{t}_l - e^{-i\hat{\varphi}_l}\hat{r}_l\}, \tag{47}$$

where $\hat{\varphi}_l = \hat{p}_l d_l$, d_l is the layer thickness. The set of these equations should, as usual, be completed by adding two more boundary conditions: one for the front interface with the vacuum and a second one for the back interface N with the substrate:

$$\hat{1} + \hat{R} = \hat{t}_1 + \hat{r}_1, \tag{48}$$

$$p_0(\hat{1} - \hat{R}) = \hat{p}_1(\hat{t}_1 - \hat{r}_1), \tag{49}$$

$$\hat{T} = e^{i\hat{\varphi}_N}\hat{t}_N + e^{-i\hat{\varphi}_N}\hat{r}_N, \tag{50}$$

$$\hat{p}_s\hat{T} = \hat{p}_N(e^{i\hat{\varphi}_N}\hat{t}_N - e^{-i\hat{\varphi}_N}\hat{r}_N), \tag{51}$$

where the wave number operator in the substrate is denoted as $\hat{p}_s$.

The set of Eqs.(46-51) looks exactly the same as those for spin–less particles and the only difference is that each of the equation is written for 2×2 matrices, i.e. actually represents a couple of equations. However, one should not pay too much attention to this fact and can obtain solutions of the system of Eqs.(48-51) for the reflectance, $\hat{r}_l$, and transmittance, $\hat{t}_l$ matrices, including $\hat{R}$ and $\hat{T}$.

One of the ways to find solutions is to apply a customarily used matrix formalism[5] and express each couple of Eqs.(46-47) as one (super-)matrix equation:

$$\begin{pmatrix} (\hat{t}_{l+1} + \hat{r}_{l+1}) \\ i(\hat{t}_{l+1} - \hat{r}_{l+1}) \end{pmatrix} = \hat{\hat{S}}_l \begin{pmatrix} (\hat{t}_l + \hat{r}_l) \\ i(\hat{t}_l - \hat{r}_l) \end{pmatrix}, \tag{52}$$

where the supermatrices $\hat{\hat{S}}_l$:

$$\hat{\hat{S}}_l = \begin{pmatrix} \hat{S}_l^{11} & \hat{S}_l^{12} \\ \hat{S}_l^{21} & \hat{S}_l^{22} \end{pmatrix} = \begin{pmatrix} \cos\hat{\varphi}_l & \hat{p}_l^{-1}\sin\hat{\varphi}_l \\ -\hat{p}_l\sin\hat{\varphi}_l & \cos\hat{\varphi}_l \end{pmatrix}, \tag{53}$$

are built up of four 2×2 matrices $\hat{S}_l = S_l^{\alpha\beta}$, with $\alpha = 1, 2$, $\beta = 1, 2$.

A particular advantage of Eq.(52) is that one can consequently apply it starting from the front face down to the interface with the substrate and finally obtain a closed form equation for the reflectance, $\hat{R} = \hat{r}_0$ and transmittance, $\hat{T} = \hat{t}_N$ matrices:

$$\begin{pmatrix} \hat{T} \\ i\hat{T} \end{pmatrix} = \hat{\hat{S}} \begin{pmatrix} (\hat{1} + \hat{R}) \\ i(\hat{1} - \hat{R}) \end{pmatrix}, \tag{54}$$

with the super–matrix $\hat{\hat{S}}$ defined as product

$$\hat{\hat{S}} = \hat{\hat{S}}_0 \times \hat{\hat{S}}_1 \times ... \times \hat{\hat{S}}_N = \hat{\hat{S}} = \begin{pmatrix} \hat{S}^{11} & \hat{S}^{12} \\ \hat{S}^{21} & \hat{S}^{22} \end{pmatrix}. \tag{55}$$

Solving two Eq.(54) with respect to the two unknown matrices $\hat{T}$ and $\hat{R}$, one immediately obtains them in explicit form:

$$\hat{R} = \tfrac{1}{2}\{(\hat{S}^{11} - \hat{S}^{21}) + (\hat{S}^{12} - \hat{S}^{22})\hat{p}_s/p_0\}\hat{T} \quad , \tag{56}$$

$$\hat{T} = 2\{(\hat{S}^{11} + \hat{S}^{21}) + (\hat{S}^{12} + \hat{S}^{22})\hat{p}_s/p_0\}^{-1}. \tag{57}$$

Then the only problem left is to compute the elements $\hat{S}^{\alpha\beta}$ of the total supermatrix $\hat{\hat{S}}$. As usual in super–matrix multiplication one should make it in two steps. In the first step matrix elements are $\hat{S}^{\alpha\beta}$ of the supermatrix $\hat{\hat{S}}$ are to be considered as c–numbers, but without changing the order in which they are disposed in the product so, that

$$\hat{S}^{\alpha\beta} = \sum_{\alpha_1\alpha_2...\alpha_N=1,2} \hat{S}_0^{\alpha\alpha_1}\hat{S}_1^{\alpha_1\alpha_2}....S_N^{\alpha_N\beta} \tag{58}$$

In the second step, one must follow an usual rule for multiplication of the matrices in each term of this sum.

The matrix elements $\hat{S}_l^{\alpha\beta}$ can easily be found using the theorem formulated in Eq.(29), according to which:

$$\hat{S}_l^{\alpha\beta} \;=\; \frac{1}{2}\{\hat{1}(S_{l+}^{\alpha\beta} + S_{l-}^{\alpha\beta}) + (\hat{\boldsymbol{\sigma}}\mathbf{b}_l)(S_{l+}^{\alpha\beta} - S_{l-}^{\alpha\beta})\}, \tag{59}$$

or explicitly in the laboratory coordinate system:

$$\hat{S}_l^{\alpha\beta} = \frac{1}{2}\begin{pmatrix} S_{l+}^{\alpha\beta}(1+b_{lz}) + S_{l-}^{\alpha\beta}(1-b_{lz}) & (S_{l+}^{\alpha\beta} - S_{l-}^{\alpha\beta})(b_{lx} - ib_{ly}) \\ (S_{l+}^{\alpha\beta} - S_{l-}^{\alpha\beta})(b_{lx} + ib_{ly}) & S_{l+}^{\alpha\beta}(1-b_{lz}) + S_{l-}^{\alpha\beta}(1+b_{lz}) \end{pmatrix}, \tag{60}$$

where the matrix elements elements $S_{\pm}^{\alpha\beta}$ are as follows:

$$S_{l\pm}^{11} \;=\; S_{l\pm}^{22} = \cos\varphi_{l\pm} \tag{61}$$

$$S_{l\pm}^{12} \;=\; p_{l\pm}^{-1}\sin\varphi_{l\pm} \tag{62}$$

$$S_{l\pm}^{21} \;=\; -p_{l\pm}\sin\varphi_{l\pm}, \tag{63}$$

and $\varphi_{l\pm} = p_{l\pm}d_l$.

Inspite of a certain elegancy of the SM routine it is "ill-conditioned" and may cause numerical problems for a large number, or/and thicknesses of the layers. The source of the

problems is rather evident and related to the imaginary phases $\varphi_{l\pm}$ in Eqs.(61–63) (or to their sum over the multilayer) which may become large below the total reflection edge. Then $\sin\varphi_{\pm}$ and $\cos\varphi_{\pm}$ contains a huge exponent, which must finally be canceled in the equations for the reflectance and transmittance. It is a quite difficult to resolve the problem within the frame of SM, but much easier to cure in the generalized Parratt formalism[8], which is based on the same principles, as the matrix routine, although uses another algorithm of calculations. In fact, the matrix Eqs.(46,47) can be immediately solved with respect to the ratio $\hat{R}_l = (\hat{r}_l\hat{t}_l^{-1})$ written as:

$$\hat{R}_l = \mathrm{e}^{i\hat{\varphi}_l}\{(\hat{1} - \hat{p}_l^{-1}\hat{p}_{l+1}) + (\hat{1} + \hat{p}_l^{-1}\hat{p}_{l+1})\hat{R}_{l+1}\}\{(\hat{1} + \hat{p}_l^{-1}\hat{p}_{l+1}) + (\hat{1} - \hat{p}_l^{-1}\hat{p}_{l+1})\hat{R}_{l+1}\}^{-1}\mathrm{e}^{i\hat{\varphi}_l}. \quad (64)$$

These equations can be easily solved via recursion, beginning from the values $\hat{R}_{N+1} = 0$ and ending by $\hat{R}_0 = \hat{R}$. Then the transmittance matrices are computed via the recursive solution of the following set of equations:

$$\hat{t}_{l+1} = \{\hat{1} + \hat{R}\}^{-1}\{\hat{1} + \mathrm{e}^{i\hat{\varphi}_l}\hat{R}_l\mathrm{e}^{i\hat{\varphi}_l}\}\mathrm{e}^{i\hat{\varphi}_l}\hat{t}_l. \quad (65)$$

The recursion begins with $\hat{t}_0 = \hat{1}$ and ends with $\hat{t}_{N+1} = \hat{T}$. The reflectance matrices are $\hat{r}_l = \hat{R}_l\hat{t}_l$ are computed via $\hat{R}_l$ and $\hat{t}_l$. In analogue to SM this method may be called Super–Recursion (SR), or Matrix-Recursion (MR) formalism, because it uses recursion routine for solution of coupled matrix equations. The recursion elements contains only decaying exponents and to the best of our experience the routine never causes numerical problems.

9.6 specular reflectivity

In accordance with Eq.(40) the reflectance matrix transforms the spin components of the incoming neutron $|\psi^i(0)\rangle$ into the components of reflected wave $|\psi^f(0)\rangle = \hat{R}|\psi^i(0)\rangle$ in the immediate vicinity of the surface. In this range $|\psi^i(0)\rangle = \hat{\mathcal{S}}_0^i|\psi_0^i\rangle$ is determined by the initial state of neutron $|\psi_0^i\rangle$ within the source developed by the $\hat{\mathcal{S}}_0^i-$ matrix governing its propagation to the surface. As it was discussed above, the observable quantities are the result of averaging over the states of the source. The reflected wave propagates to the analyzing system and one observes a result of its interaction with the detector. The amplitude of this interaction is given by the projection $\langle\psi_0^f|\hat{\mathcal{S}}_0^f|\psi^f(0)\rangle$ of the reflected wave states $\hat{\mathcal{S}}_0^f|\psi^f(0)\rangle$ driven to the analyzer by the $\hat{\mathcal{S}}_0^f-$matrix onto the analyzer eigenstates $\langle\psi_0^f|$. The analyzing system, as well as the source of polarized neutrons, is a statistical device and the result of

the interaction of the wave with the analyzer (including detector) should be averaged over its states. If on the way from the source to the analyzer the wave states do not change, then the result of this interaction just consists in the projection of the vector of states of the reflected wave onto the vector of states $|\psi_0^f\rangle$. Generally, the measurable reflectivity $\mathcal{R}$ is given by the expectation value:

$$\mathcal{R} = \overline{|\langle\psi_0^f|\mathcal{S}_0^{f+}\hat{R}\mathcal{S}_0^i|\psi_0^i\rangle|^2} = \mathrm{Tr}\{\hat{\rho}_f\hat{R}\hat{\rho}_i\hat{R}^+\}, \tag{66}$$

$$\hat{\rho}_i = \hat{\mathcal{S}}_0^i\overline{|\psi_0^i\rangle\langle\psi_0^i|}\hat{\mathcal{S}}_0^{i+} = \hat{\mathcal{S}}_0^i\hat{\rho}_0^i\hat{\mathcal{S}}_0^{i+}, \tag{67}$$

$$\hat{\rho}_f = \hat{\mathcal{S}}_0^{f+}\overline{|\psi_0^f\rangle\langle\psi_0^f|}\hat{\mathcal{S}}_0^f = \hat{\mathcal{S}}_0^{f+}\hat{\rho}_0^f\hat{\mathcal{S}}_0^f, \tag{68}$$

where $\hat{\rho}_0^i$ and $\hat{\rho}_0^f$ are the density matrices of the polarizer (source) and analyzer (detector), respectively

$$\hat{\rho}_0^i = \frac{1}{2}(\hat{1} + \mathbf{P}_0^i\hat{\boldsymbol{\sigma}}), \tag{69}$$

$$\hat{\rho}_0^f = \frac{1}{2}(\hat{1} + \mathbf{P}_0^f\hat{\boldsymbol{\sigma}}), \tag{70}$$

$\mathbf{P}_0^i$ is the vector of initial polarization, and $\mathbf{P}_0^f$ is the vector of polarization efficiency of the analyzer.

The effective density matrices at the sample surface are written in the same form:

$$\hat{\rho}_i = \frac{1}{2}(\hat{1} + \mathbf{P}_i\hat{\boldsymbol{\sigma}}), \tag{71}$$

$$\hat{\rho}_f = \frac{1}{2}(\hat{1} + \mathbf{P}_f\hat{\boldsymbol{\sigma}}), \tag{72}$$

via the corresponding vectors $\mathbf{P}_i$, calculated in Eqs.(23,24) and $\mathbf{P}_f$ defined in the same manner.

The reflectance matrix, as any 2×2 matrix, can generally be represented in a form similar to Eqs.(69-72) :

$$\hat{R} = (R\hat{1} + \mathbf{R}\hat{\boldsymbol{\sigma}}), \tag{73}$$

where $R = \frac{1}{2}\mathrm{Tr}\{\hat{R}\}$, and $\mathbf{R} = \frac{1}{2}\mathrm{Tr}\{\hat{R}\hat{\boldsymbol{\sigma}}\}$.

After substitution of this equation into Eq.(66) and calculating the traces, one can obtain[6] the following final equation for the reflectivity

$$\begin{aligned}\mathcal{R} = {} & \tfrac{1}{2}\{|R|^2[1 + (\boldsymbol{P}_i\boldsymbol{P}_f)] + |\boldsymbol{R}|^2[1 - (\boldsymbol{P}_i\boldsymbol{P}_f)]\} \\ & + \Re\{R^*(\boldsymbol{R}[\boldsymbol{P}_i + \boldsymbol{P}_f]) + (\boldsymbol{R}^*\boldsymbol{P}_i)(\boldsymbol{R}\boldsymbol{P}_f)\} \\ & - \Im\{R^*(\boldsymbol{R}[\boldsymbol{P}_i \times \boldsymbol{P}_f]) + \tfrac{1}{2}(\boldsymbol{P}_i - \boldsymbol{P}_f)[\boldsymbol{R}^* \times \boldsymbol{R}]\}.\end{aligned} \tag{74}$$

This equation, together with the procedure of calculation of the reflectance matrix $\hat{R}$, totally solve the problem to compute all spin-flip and non-spin-flip reflectivities for an arbitrary orientation between the initial polarization and the polarization analysis vector from layered systems with any distribution of the magnetization distribution over different layers. This equation is absolutely exact and general. It does not imply approximations. It is also valid for the transmission coefficient, if one just substitutes reflectance, $\hat{R}$, for transmittance, $\hat{T}$, matrices. In that sense it generalizes the consideration above for the Larmor precession.

Moreover, due to the vectorial form of Eq.(74), it can easily be averaged over the magnetization directions in multidomain samples, if the domain sizes are greater, then the lateral projection of the coherence length. Then, one can also compute the depolarization in inhomogeneously varied field along the beam path, just considering transmission through the field range divided into set of slices as discussed above. This allows to account for not only depolarization due to the LP de-phasing, as discussed above, but also depolarization caused by the lost intensity due to the reflection. The latter mechanism of depolarization is similar to that due to the scattering[1] beyond aperture on the analyzing system.

The limitation of Eq.(74) is only the coherence length. If it is greater than the typical size of magnetic inhomogeneities, then the wave is not only reflected from and transmitted through the mean optical potential, but also scattered in off-specular directions. This phenomenon is considered in the next Section.

9.7 scattering cross section

The reflectivity $\mathcal{R}$ is a dimensionless quantity, normalized to the flux incoming onto the sample surface. One can also introduce the cross section of specular reflection,

$$\left(\frac{d\sigma}{d\Omega}\right)_r = (2\pi)^2 \mathcal{R}(q_\perp)\delta(\mathbf{q}_\parallel) \tag{75}$$

which describes a flux divergent from the image of the source mirrored with respect to the surface plane. The cross section has the dimension of an area and the $\delta-$ function explicitly accounts for the conservation of the lateral projection of the wave vector: no lateral momentum transfer $\mathbf{q}_\parallel = \boldsymbol{\kappa}_f - \boldsymbol{\kappa}_i$ is allowed for an interaction with an infinite surface, and the transverse momentum transfer $q_\perp = p_{0f} \pm p_{0i}$ for reflection is $q_\perp = 2p_{0i}$. The effect of the finite coherence length is accounted for via smearing of Eq.(75) over the resolution function.

The advantage of Eq.(75) is that the measured reflected flux can be compared with flux

scattered in off–specular directions due to heterogeneities smaller than the coherence length. The scattering cross section is defined as a modulus of the scattering amplitude $\hat{\mathcal{F}}(\mathbf{k}_f;\mathbf{k}_i)$ squared

$$\frac{d\sigma}{d\Omega} = \overline{\langle|\hat{\mathcal{F}}(\mathbf{k}^f,\mathbf{k}^i)|^2\rangle}, \tag{76}$$

and averaged over the spin states of the source and the analyzer of scattering signal. In general, the scattering cross section depends not on the momentum transfer $\mathbf{q} = \mathbf{k}_f - \mathbf{k}_i$, or its components, as in Eq.(75), but is a function of two vector variables, i.e. of the incoming, $\mathbf{k}_i$, and outgoing, $\mathbf{k}_f$, wave vectors.

The scattering amplitude operators $\hat{\mathcal{F}} = \mathcal{F}(\hat{\boldsymbol{\sigma}})$ in Eq.(76) are scalar functions of the vector of Pauli matrices and thanks to the theorem in Eq.(29) are generally represented as linear functions

$$\hat{\mathcal{F}} = \hat{1}\mathcal{F}_0 + (\boldsymbol{\mathcal{F}}\hat{\boldsymbol{\sigma}}), \tag{77}$$

with $\mathcal{F}_0 = \frac{1}{2}\mathrm{Tr}\{\hat{\mathcal{F}}\hat{\boldsymbol{\sigma}}\}$, and $\boldsymbol{\mathcal{F}} = \frac{1}{2}\mathrm{Tr}\{\hat{\mathcal{F}}\hat{\boldsymbol{\sigma}}\}$.

Then, after accomplishing the averaging procedure similar to the case of reflectivity the equation for the scattering cross section:

$$\frac{d\sigma}{d\Omega} = \mathrm{Tr}\{\hat{\rho}_f\hat{\mathcal{F}}\hat{\rho}_i\hat{\mathcal{F}}^+\} \tag{78}$$

boils down to the form

$$\begin{aligned}\tfrac{d\sigma}{d\Omega} = \tfrac{1}{2}\{|\mathcal{F}_0|^2[1+(\boldsymbol{P}_i\boldsymbol{P}_f)] + |\boldsymbol{\mathcal{F}}|^2[1-(\boldsymbol{P}_i\boldsymbol{P}_f)]\} \\ +\Re\{\mathcal{F}_0^*(\boldsymbol{\mathcal{F}}[\boldsymbol{P}_i+\boldsymbol{P}_f]) + (\boldsymbol{\mathcal{F}}^*\boldsymbol{P}_i)(\boldsymbol{\mathcal{F}}\boldsymbol{P}_f)\} \\ -\Im\{\mathcal{F}_0^*(\boldsymbol{\mathcal{F}}[\boldsymbol{P}_i\times\boldsymbol{P}_f]) + \tfrac{1}{2}(\boldsymbol{P}_i-\boldsymbol{P}_f)[\boldsymbol{\mathcal{F}}^*\times\boldsymbol{\mathcal{F}}]\},\end{aligned} \tag{79}$$

which exactly coincides with that in Eq.(74), if one substitutes $\mathcal{F}_0$ by $R = R(q_\perp)$ and $\boldsymbol{\mathcal{F}}$ is exchanged for $\boldsymbol{R} = \boldsymbol{R}(q_\perp)$.

If the scattering is weak, then in the Born Approximation (BA) $\mathcal{F}_0$ and $\boldsymbol{\mathcal{F}}$ are purely real functions of the wave vector transfer $\boldsymbol{q} = \boldsymbol{k}_f - \boldsymbol{k}_i$, $\boldsymbol{\mathcal{F}}$ is directed along the vector $\boldsymbol{B}(\boldsymbol{q}) = \boldsymbol{M} - \boldsymbol{e}(\boldsymbol{e}\boldsymbol{M})$, $\boldsymbol{e} = \boldsymbol{q}/|\boldsymbol{q}|$, and Eq.(79) collapses to the corresponding equations in Ref.(1).

Beyond the BA, $\mathcal{F}$ and $\boldsymbol{\mathcal{F}}$ are, in general, complex functions and, for example, the last terms in Eq.(79) survive. One of the examples when one must go systematically beyond the

BA, even if scattering is weak, is off–specular scattering at grazing incidence. Then one must account for the optical effects, e.g. the distortions due to the refraction (birefringence) of the incident and scattered waves, as well as due to the off–specular scattering of the waves reflected from the mean optical potential averaged over the lateral coherence length.

9.8 Distorted Wave Born Approximation (DWBA)

DWBA[18] represents a typical example of the perturbation theory approach which generally implies to use an exact solution of the simplified reference Hamiltonian as a starting point for iteration over the difference between this Hamiltonian and that to be solved. The iteration procedure may not converge to the correct solution, or even not converge to any other. However, for a proper choice of the reference Hamiltonian already a few first iterations usually give a result that is assumed, as being reasonably close to the exact solution of the problem, if the perturbation parameter is small. In most of the cases only the first iteration is accounted for. Thus, the BA uses the reference Hamiltonian for waves that are freely propagating before and after a scattering event. In the form of DWBA suggested by Sinha et al.[11] for the X-ray off–specular scattering the zero approximation assumes an exact solution of the Schrödinger equation for the reflection potential, while the residual potential is treated as a perturbation. In our case the operator (in the spin space) $\hat{V}(z)$ responsible for optical effects is given in Eq.(38), and the zero order solution for the vector of states,

$$|\Psi^i(\mathbf{r})\rangle = \exp(i\boldsymbol{\kappa}\boldsymbol{\rho}) \sum_l \hat{\mathcal{S}}_{li}(z, \boldsymbol{\sigma})|\psi^i(0)\rangle, \tag{80}$$

is found, if the transmittances $\hat{t}_l$ and reflectances, $\hat{r}_l$, in Eq.(43) are computed via, say, SM, or SR routine.

The exact vector of states in the presence of scattering is to be represented as a sum

$$|\Psi(\mathbf{r})\rangle = |\Psi^i(\mathbf{r})\rangle + |\Psi_s(\mathbf{r})\rangle, \tag{81}$$

where the vector $|\Psi_s(\mathbf{r})\rangle$ describes the scattered wave, caused by the residual perturbation operator, which is

$$\hat{\mathcal{V}}(\mathbf{r}) = \hat{V}(\mathbf{r}) - \hat{V}(z), \tag{82}$$

where $\langle\hat{\mathcal{V}}(\mathbf{r})\rangle_{\boldsymbol{\rho}} = 0$ and does not contribute to the specular reflection.

Substitution of Eq.(82) into Eq.(25) allows to re-write it in a form ready for iterations:

$$\{\hat{1}(\hbar^2/2m)[\nabla^2 + k_0^2] - \hat{V}(z)\}|\Psi_s(\mathbf{r})\rangle = \hat{\mathcal{V}}(\mathbf{r})\{|\Psi^i(\mathbf{r})\rangle + |\Psi_s(\mathbf{r})\rangle\}, \tag{83}$$

where the right hand side of the equation can be considered as an effective source of scattered particles.

The formal solution of this equation, or better to say, its integral form reads:

$$|\Psi_s(\mathbf{r})\rangle = (2m/\hbar^2)\int \mathrm{d}\mathbf{r}'\hat{G}(\mathbf{r},\mathbf{r}')\hat{\mathcal{V}}(\mathbf{r}')\{|\Psi^i(\mathbf{r}')\rangle + |\Psi_s(\mathbf{r}')\rangle\}, \tag{84}$$

where $\hat{G}(\mathbf{r},\mathbf{r}')$ is the 2×2 matrix Green function, which obeys the same equation, but for a point-like source, i.e. with the right hand side term in Eq.(84) substituted for $\hat{1}\delta(\mathbf{r}-\mathbf{r}')$.

A formal solution of Eq.(84) has a standard form:

$$\hat{G}(\mathbf{r},\mathbf{r}') = \hat{G}_0(\mathbf{r}-\mathbf{r}') + \int \mathrm{d}\mathbf{r}_1\hat{G}_0(\mathbf{r}-\mathbf{r}_1)\hat{V}(z_1)\hat{G}(\mathbf{r}_1,\mathbf{r}'), \tag{85}$$

where $\hat{G}_0(\mathbf{r}-\mathbf{r}')$ is the matrix Green function in empty space, i.e. the well known solution of Eq.(84) at $\hat{V}(z)=0$ and the $\delta-$function in the right hand side. This solution is nothing else that a spherical wave divergent from the source position:

$$\hat{G}_0(\mathbf{r}-\mathbf{r}_1) = \frac{\hat{1}m}{2\pi\hbar^2}\frac{\mathrm{e}^{\mathrm{i}k_0|\mathbf{r}-\mathbf{r}_1|}}{|\mathbf{r}-\mathbf{r}_1|} \approx \hat{G}_0(\mathbf{r})\mathrm{e}^{-\mathrm{i}\mathbf{k}\mathbf{r}_1}. \tag{86}$$

Here the right hand side approximation holds for $r \gg r_1$, and $\mathbf{k} = k_0\mathbf{r}/r$. Substitution of this approximate form of $\hat{G}_0(\mathbf{r}-\mathbf{r}_1)$ into Eq.(85) allows to write down a very useful equation for the total matrix Green function $\hat{G}(\mathbf{r},\mathbf{r}')$:

$$\hat{G}(\mathbf{r},\mathbf{r}') = \hat{G}_0(\mathbf{r})\{\hat{1}\mathrm{e}^{-\mathrm{i}\mathbf{k}\mathbf{r}'} + \int \mathrm{d}\mathbf{r}_1\mathrm{e}^{-\mathrm{i}\mathbf{k}\mathbf{r}_1}\hat{V}(z_1)\hat{G}(\mathbf{r}_1,\mathbf{r}')\}. \tag{87}$$

Projection of this equation and Eq.(84) onto the vector of final states $\langle\Psi_0^f|$ immediately provides the solution for the scattering amplitude in the DWBA:

$$\mathcal{F}(\mathbf{k}^f,\mathbf{k}^i) = \langle\psi_0^f|\Psi_s(\mathbf{r})\rangle = -\frac{m}{2\pi\hbar^2}\int \mathrm{d}\mathbf{r}\langle\Psi^f(\mathbf{k}^f,\mathbf{r})|\hat{\mathcal{V}}(\mathbf{r})|\Psi^i(\mathbf{k}^i,\mathbf{r})\rangle, \tag{88}$$

if in the first order of the DWBA the second term in Eq.(84) is neglected.

This equation can be re-written in a more suitable form:

$$\mathcal{F}(\mathbf{k}^f,\mathbf{k}^i) = -\frac{m}{2\pi\hbar^2}\int \mathrm{d}\mathbf{r}\langle\psi_0^f|\hat{\mathcal{S}}^f(\mathbf{r})\hat{\mathcal{V}}(\mathbf{r})\hat{\mathcal{S}}^i(\mathbf{r})|\psi_0^i\rangle, \tag{89}$$

taking into account that the vector of states $|\Psi^i(\mathbf{r})\rangle = \hat{\mathcal{S}}^i|\psi_0^i\rangle$ and $\langle\Psi^f(\mathbf{r})| = \langle\psi_0^f|\hat{\mathcal{S}}^i$ are transformed by the corresponding $\hat{\mathcal{S}}-$matrices.

The latter obey the Schrödinger equations:

$$\hat{\mathcal{S}}^i(\mathbf{r}) = \hat{\mathcal{S}}_0^i(\mathbf{r}) + \int \mathrm{d}\mathbf{r}_1\hat{\mathcal{S}}^i(\mathbf{r}_1)\hat{V}(z_1)\hat{G}_0(\mathbf{r}_1,\mathbf{r}) \tag{90}$$

$$\hat{\mathcal{S}}^f(\mathbf{r}) = \hat{\mathcal{S}}_0^f(\mathbf{r}) + \int \mathrm{d}\mathbf{r}_1\hat{G}_0(\mathbf{r},\mathbf{r}_1)\hat{V}(z_1)\hat{\mathcal{S}}^f(\mathbf{r}_1) \tag{91}$$

where $\hat{\mathcal{S}}_0^i(\mathbf{r}) = \hat{1}\exp(\mathrm{i}\mathbf{k}^i\mathbf{r})$, and $\hat{\mathcal{S}}^f(\mathbf{r}) = \hat{1}\exp(-\mathrm{i}\mathbf{k}^f\mathbf{r})$ are the solutions with $\hat{\mathcal{V}}(z) = 0$. Eqs.(90, 91) include different asymptotic conditions: Eq.(90) assumes that the wave approaches the sample from the direction of the source, whereas due to the asymptotic conditions, Eq.(91) anticipates that the wave approaches the sample from the side of the analyzer. Hence $\mathbf{k}^i$ and $\mathbf{k}^f$ are incoming and, correspondingly, outgoing wave vectors, the matrix element Eq.(89) contains the incoming vector of states $|\Psi^i(\mathbf{r})\rangle$, whereas $\langle\Psi^f(\mathbf{r})|$, corresponds to the vector of states inverted is space, rather than reversed in time[11], with respect to that describing the outgoing wave.

Due to the conservation in Eqs.(90,91) of the lateral projections $\boldsymbol{\kappa}^i$ and $\boldsymbol{\kappa}^f$ projections of the wave vectors, $\mathbf{k}^i$, and correspondingly, $\mathbf{k}^f$, the solutions of Eqs.(89,90) are written in the factorized form:

$$\hat{\mathcal{S}}^i(\mathbf{r}) = \exp(\mathrm{i}\boldsymbol{\kappa}^i\boldsymbol{\rho})\hat{\mathcal{S}}^i(z), \quad \text{and} \quad \hat{\mathcal{S}}^f(\mathbf{r}) = \exp(-\mathrm{i}\boldsymbol{\kappa}^f\boldsymbol{\rho})\hat{\mathcal{S}}^f(z), \tag{92}$$

where $\mathcal{S}^i(z) = \mathcal{S}^i(p_0^i, z)$, for scattering into the upper hemisphere $\mathcal{S}^f(z) = \mathcal{S}^f(p_0^f, z)$, while for scattering below the horizon $\mathcal{S}^f(z) = \mathcal{S}^f(-p_0^f, z)$.

Now, Eq.(89) is written in the form taking into account the lateral translational invariance of the reference state:

$$\mathcal{F}(\mathbf{q}_\parallel; p_0^f, p_0^i) = -\frac{m}{2\pi\hbar^2}\int \mathrm{d}z \int \mathrm{d}\boldsymbol{\rho}\mathrm{e}^{-\mathrm{i}\mathbf{q}_\parallel\boldsymbol{\rho}}\langle\psi_0^f|\hat{\mathcal{S}}^f(z)\hat{\mathcal{V}}(\mathbf{r})\hat{\mathcal{S}}^i(z)|\psi_0^i\rangle, \tag{93}$$

where $\mathbf{q}_\parallel = \boldsymbol{\kappa}^f - \boldsymbol{\kappa}^i$ is the lateral momentum transfer.

The matrices $\hat{\mathcal{S}}^i(z)$ and $\hat{\mathcal{S}}^f(z)$ depend only on $z-$coordinate and can be found for almost arbitrary $V(z)$ profiles by solving the equations following from Eqs.(90,91):

$$\hat{\mathcal{S}}^i(z) = \hat{\mathcal{S}}_0^i(z) + \int \mathrm{d}z_1\hat{\mathcal{S}}^i(z_1)\hat{V}(z_1)\hat{G}_0(z_1 - z), \tag{94}$$

$$\hat{\mathcal{S}}^f(z) = \hat{\mathcal{S}}_0^f(z) + \int \mathrm{d}z_1\hat{G}_0(z - z_1)\hat{V}(z_1)\hat{\mathcal{S}}^f(z_1), \tag{95}$$

in which the Green function $\hat{G}_0(p_0, z_1 - z)$ of free propagation is defined via the Fourier transform of the left hand side part of Eq.(86):

$$\hat{G}_0(z_1 - z) = -\hat{1}\frac{\mathrm{i}m}{\hbar p_0}\mathrm{e}^{\mathrm{i}p_0|z_1 - z|}. \tag{96}$$

Here p_0 has a meaning of either the transverse component $p_0^i = k_0\sin\alpha_i$ of the wave vector $\mathbf{k}^i$, or corresponding component $p_0^f = k_0\sin\alpha_f$ of the vector $\mathbf{k}^f$.

One of the ways to solve Eqs.(94, 95) is divide the space along the $z-$axis into a set of intervals, numerated by $1 < l < N$ and such, that and in each of them one can neglect

variation of the potential $V(z)$. Then one can represent the solution for $\hat{\mathcal{S}}_l^i(z)$ and $\hat{\mathcal{S}}_l^f(z)$ within each of those intervals similar to that given in Eq.(43), but with $\hat{t}$ substituted for $\hat{t}_l^i$, or t_l^f, $\hat{r}$ substituted for $\hat{i}_l^i$, or $\hat{r}_l^f$, and $\varphi_l(z)$ substituted exchanged for $\hat{\varphi}_l^{i(f)} = \hat{p}_l^{i(f)}(z - z_{l-1})$, where $p_l^{i(f)}$ are defined in the same manner as in Eq.(43), but with p_0 substituted for p_0^i, or p_0^f, respectively.

Finally the scattering amplitude in DWBA is proportional to the sum of matrix elements:

$$\mathcal{F}(\mathbf{q}_\parallel; p_{0f}, p_{0i}) = \sum_l \int \mathrm{d}z \langle \psi_0^f | \hat{\mathcal{S}}_l^f(z) \hat{\mathcal{F}}_l(\mathbf{q}_\parallel; z) \hat{\mathcal{S}}_l^i(z) | \psi_0^i \rangle, \tag{97}$$

where

$$\hat{\mathcal{F}}_l(\mathbf{q}_\parallel; z) = \frac{m}{2\pi\hbar^2} \int \mathrm{d}\boldsymbol{\rho} \mathrm{e}^{-\mathrm{i}\mathbf{q}_\parallel \boldsymbol{\rho}} \hat{\mathcal{V}}_l(\boldsymbol{\rho}, z) \tag{98}$$

In the case of lateral diffraction and off-specular scattering at low incident angles one can perform integration over the lateral coordinates in this equation. Then the scattering matrix is written as a product:

$$\hat{\mathcal{F}}_l(\mathbf{q}_\parallel; p^f, p^i) = \Lambda_l(\mathbf{q}_\parallel) \hat{F}_l(\mathbf{q}_\parallel; p^f, p^i) \tag{99}$$

$$\Lambda_l(\mathbf{q}_\parallel) = \sum_j \mathrm{e}^{i\mathbf{q}_\parallel \boldsymbol{\rho}_j^l}, \tag{100}$$

where $\boldsymbol{\rho}_j^l$ are the lateral coordinates of atoms within l^{th} layer, or slice. Assuming, that at $p_0^{i,f} \ll a_{l\perp}^{-1}$, where $a_{l\perp}$ is the unit cell constant in the direction perpendicular to the surface, one can write down an equation for $\hat{F}_l^{if} = \hat{F}_l(\mathbf{q}_\parallel; p^i, p^f)$ as follows:

$$\hat{F}_l^{fi} = \frac{1}{d_l} \int_0^{d_l} \hat{\mathcal{S}}_l^f(z) \hat{F}_l(\mathbf{q}_\parallel) \hat{\mathcal{S}}_l^i(z). \tag{101}$$

where $\hat{\mathcal{S}}_l(z)$–matrices are given in Eq.(43), $\hat{F}_l(\mathbf{q}_\parallel) = \hat{F}_l(\mathbf{q}_\parallel, 0) \approx \hat{F}_l(\mathbf{q})$, and

$$\hat{F}_l(\mathbf{q}) = F_{Nl}(\mathbf{q}) + (\boldsymbol{\sigma} \mathbf{m}_{l\perp}) F_{Ml}(\mathbf{q}). \tag{102}$$

In Eq.(101) $F_{Nl} = b_{Nl} \mathcal{F}_{Nl}(\mathbf{q})$ is a product of the nuclear scattering length b_{Nl} and the nuclear structure factor $\mathcal{F}_{Nl}(\mathbf{q})$, while $F_{Ml} = b_{Ml} \mathcal{F}_{Ml}(\mathbf{q})$ is a product of the magnetic scattering length b_{Ml} and the magnetic cell form factor $\mathcal{F}_{Ml}(\mathbf{q})$, $\mathbf{m}_{l\perp} = \mathbf{m}_l - \mathbf{e}(\mathbf{e}\mathbf{m}_l)$ is the component of the unit vector $\mathbf{m}_l = \mathbf{M}_l / M_l$ perpendicular to the momentum transfer direction given by the unit vector $\mathbf{e} = \mathbf{q}/|\mathbf{q}|$.

Substitution of Eqs.(43,102) into Eq.(100) yields:

$$\hat{F}_l^{fi} = \tfrac{1}{4}\{G_{l++}[1+\boldsymbol{\sigma}\mathbf{b}_l]\hat{F}_l(\mathbf{q})[1+\boldsymbol{\sigma}\mathbf{b}_l]$$
$$+G_{l+-}[1+\boldsymbol{\sigma}\mathbf{b}_l]\hat{F}_l(\mathbf{q})[1-\boldsymbol{\sigma}\mathbf{b}_l]$$
$$+G_{l-+}[1-\boldsymbol{\sigma}\mathbf{b}_l]\hat{F}_l(\mathbf{q})[1+\boldsymbol{\sigma}\mathbf{b}_l]$$
$$+G_{l--}[1-\boldsymbol{\sigma}\mathbf{b}_l]\hat{F}_l(\mathbf{q})[1-\boldsymbol{\sigma}\mathbf{b}_l]\}, \tag{103}$$

where $G_{l\mu\nu} = G^{fi}_{l\mu\nu}$, $\mu = \pm$, $\nu = \pm$, and

$$G^{fi}_{l\mu\nu} = t^f_{l\mu}t^i_{l\nu}g^{tt}_{l\mu\nu} + r^f_{l\mu}r^i_{l\nu}g^{rr}_{l\mu\nu} + r^f_{l\mu}t^i_{l\nu}g^{rt}_{l\mu\nu} + t^f_{l\mu}r^i_{l\nu}g^{tr}_{l\mu\nu},$$
$$g^{tt}_{l\mu\nu} = \tfrac{\exp[i(\varphi^f_{l\mu}+\varphi^i_{l\nu})]-1}{i(\varphi^f_{l\mu}+\varphi^i_{l\nu})},$$
$$g^{tr}_{l\mu\nu} = \tfrac{\exp[i(\varphi^f_{l\mu}-\varphi^i_{l\nu})]-1}{i(\varphi^f_{l\mu}-\varphi^i_{l\nu})},$$
$$g^{rr}_{l\mu\nu} = g^{tt}_{l\mu\nu}\exp[-i(\varphi^f_{l\mu}+\varphi^i_{l\nu})],$$
$$g^{rt}_{l\mu\nu} = g^{tr}_{l\mu\nu}\exp[-i(\varphi^f_{l\mu}-\varphi^i_{l\nu})], \tag{104}$$

with $\varphi^{(f,i)}_{l\mu} = p^{(f,i)}_{l\mu}d_l$.

The Laue functions $g^{tt}_{\pm\pm}$ correspond to non–spin–flip processes in which the wave with $+$ or $-$ spin projection is transmitted into the film, than scattered by inhomogeneties, and the scattered wave is transmitted out of the film. The functions $g^{rr}_{\pm\pm}$ correspond to non–spin–flip transitions between reflected waves. Each of those functions reveal two sharp maxima at $p^f_\pm + p^i_\pm = 0$. Two other functions $g^{tt}_{\pm\mp}$ and $g^{rr}_{\pm\mp}$ reach their maximum values at $p^f_\pm + p^i_\mp$ corresponding to spin-flip scattering in off–specular directions. The other Laue functions $g^{tr}_{\mu\nu}$ and $g^{rt}_{\mu\nu}$ correspond to the processes with transitions between transmitted and reflected waves. They show maxima at $p^f_\pm - p^i_\pm$ (non-spin-flip), or at $p^f_\pm - p^i_\mp$ (spin-flip).

Calculating further products of the Pauli matrices in Eqs.(103) one obtaines the equation consistent with the theorem summarized in Eq.(29):

$$\hat{F}^{fi}_l = F_l + (\mathbf{F}_l\boldsymbol{\sigma}), \tag{105}$$

where $F_l = F^{fi}_l = \mathrm{Tr}\{\hat{F}^{fi}_l\}/2$ and $\mathbf{F}_l = \mathbf{F}^{fi}_l = \mathrm{Tr}\{\boldsymbol{\sigma}\hat{F}^{fi}_l\}/2$.

It is convenient for practical purposes to re-write this equation in the coordinate system naturally related for each layer to its mean magnetic field $\mathbf{B}_l$. This coordinate system can be fixed choosing three orthogonal vectors $\mathbf{b}_l = \overline{\mathbf{B}}_l/|\overline{\mathbf{B}}_l|$, $\mathbf{b}_{l\perp} = \mathbf{m}_{l\perp} - \mathbf{b}_l(\mathbf{m}_{l\perp}\mathbf{b}_l)$, and $\mathbf{b}_{la} = [\mathbf{b}_l \times \mathbf{b}_{l\perp}]$, then the vector $\mathbf{F}_l$ is decomposed as follows:

$$\mathbf{F}_l = F_{l\|}\mathbf{b}_l + F_{l\perp}\mathbf{b}_{l\perp} + F_{la}\mathbf{b}_{la}. \tag{106}$$

Finally, the zero matrix element F_l^{fi} and the components of the vector $\mathbf{F}_l^{fi}$ can be calculated and written explicitely:

$$\begin{aligned} F_l &= \frac{1}{2}\{(G_{l++}+G_{l--})F_{Nl}+(G_{l++}-G_{l--})F_{Ml}(\mathbf{b}_l\mathbf{m}_{l\perp})\}, \\ F_{l\parallel} &= \frac{1}{2}\{(G_{l++}-G_{l--})F_{Nl}+(G_{l++}+G_{l--})F_{Ml}(\mathbf{b}_l\mathbf{m}_{l\perp})\}, \\ F_{l\perp} &= \frac{1}{2}(G_{l+-}+G_{l-+})F_{Ml}, \\ F_{la} &= \frac{i}{2}(G_{l+-}-G_{l-+})F_{Ml}, \end{aligned} \tag{107}$$

where $(\mathbf{bm}_{l\perp}) = (\mathbf{bm}_l) - (\mathbf{eb}_l)(\mathbf{em}_l)$. From these equations it follows that the amplitudes F_0 and $F_\parallel$ in Eq.(98) do not contain terms responsible for transitions between the states with p_+ and p_-, while the other two, $F_\perp$ and F_a, correspond to purely magnetic scattering and provide such transitions.

If the periodical crystalline lateral structure is regarded as a perturbation, then $|\Lambda(\mathbf{q}_\parallel)|^2 = \frac{(2\pi)^2}{s_0}\mathcal{N}_0\delta(\mathbf{q}_\parallel - \boldsymbol{\tau})$, where $\boldsymbol{\tau}$ is the in–plane reciprocal vector, s_0 is the area of the unit cell cross section by the film surface, $\mathcal{N} = S_0/s_0$ and S_0 is the foot print of the beam.

In the saturated state and at the incident polarization parallel to the magnetization any spin–flip signal and, correspondingly, splitting of the diffracted beam is totally due to the local atomic field components perpendicular to the mean magnetic field direction. Then the effect is usually small due to the atomic magnetic form–factor $\mathcal{F}_M(\tau \neq 0) \ll 1$ [9]. All the considerations above are actually valid for a large domain, and in multidomain samples the scattering cross section and polarization should be averaged over domains. This will dramatically increase the spin-flip signal at specular reflection and at diffraction, but it does not increase a contribution from the two last terms in Eq.(98) responsible for the spatial splitting of the diffracted beam. If, on the contrary, there exist an amount of small domains, then the splitting is determined by the mean magnetic field, $\overline{\mathbf{B}}$ averaged over domains. It may be slightly smaller, than at saturation, but the transitions between the states with p_+ and p_- are more effeciently provided by the domain field componets perpendicular to $\overline{\mathbf{B}}$, than by the local atomic scale fields [9]. In this case magnetic scattering contributes not only into the true diffraction, but rather to diffuse scattering concentrated around the Bragg peak positions. In particular, relatively small domains (on a scale of large lateral coherence length) create low angle scattering manifested in off–specular directions. Corresponding equations have exactly the same structure as the equation for the Bragg diffraction discussed above. The only difference is that the $\delta(\mathbf{q}_\parallel - \boldsymbol{\tau})$ function should be substituted for the lateral domain

form factor $\langle|\Lambda(\mathbf{q}_\parallel)|^2\rangle_{\rm domains}$.

9.9 Example: 3D polarization anlysis

In the mean time, the reflected and scattered intensities are measured at a single direction of the initial polarization and polarization analysis, and at most four quantities: two spin–flip and two non–spin–flip components of the reflectivity (scattering cross section) are available for theoretical evaluation. However, it is well established for bulk magnetic systems that quite often measurements at one direction of the polarization do not render a sufficient amount of information needed for the unique solution of the model. More complete information is obtained from measurements at three, usually orthogonal, directions of the polarization, providing 36 instead of four experimental quantities. This technique, called Polarization Vector or 3 Dimensional (3**D**) analysis was first developed for the direct beam and small angle scattering experiments[1]. Nowadays it is used in a number of diffraction and inelastic scattering measurements, as discussed in the Lecture by F. Tasset.

In the case of reflection kinematics the situation is more complicated from both experimental and theoretical points of view. One of the main experimental problem is quite general and related to the effects of the demagnetizing field outside the sample. If this field is sufficiently homogeneous and does not lead to a noticeable spatial splitting of the neutron beam, then the Larmor precession can either be avoided by a proper short circuit for the magnetic flux outside the neutron path, or taken into account, as discussed above. In the simplest case one may analyze only the projections of the outgoing neutron spins onto the direction of incoming polarization, subsequently directed along each of three Cartesian axis. Usually, the conditions for non–adiabatic transmission of the neutron spin into the film can be fulfilled at any direction of weak field guiding the initial polarization, and this, 3–directional (according to Mezei), or 3D, version of 3**D** polarization analysis delivers 12 measurable quantities – an amount often well sufficient to define a theoretical model.

In Ref.14 the data of polarized neutron reflectivity and off–specular scattering measured for Fe/Cr multilayers were well described within the model of small antiferromagnetic domains. In these experiments the initial polarization vector $\mathbf{P}_i$ and vector of the final polarization analysis $\mathbf{P}_f$ were chosen parallel to the net magnetization of the system. Here we shall present an example of the model calculations made for forthcoming experiments on the same system, but with the vectors $\mathbf{P}_i$ and $\mathbf{P}_f$ directed also along two other axis orthogonal

to the magnetization and either parallel or perpendicular to the axis of antiferromagnetism. We shall demonstrate, that 3D analysis can deliver and additional information, which can be used to verify the model proposed in Ref.14.

In the preceding Sections the general explicit equations were derived for the reflectivity, $\mathcal{R} = \mathcal{R}(\mathbf{P}_f, \mathbf{P}_i)$, and scattering cross section, $(d\sigma/d\Omega)$, in the invariant form independent of the coordinate system and for an arbitrary mutual orientation between the vectors $\mathbf{P}_f$ and $\mathbf{P}_i$.

Now we reproduce those equations in a particular coordinate system for the model proposed in Ref.14 and depicted in Fig.1. We assume that the mean magnetization in each layer is directed along the field applied within the surface plane along the Y–axis (perpendicular to the reflection plane), and the Z–axis is orthogonal to the surface (see Fig.1). The mean magnetization $\mathbf{M}$ contributes to the specular reflection, while the components of the domain magnetic moments perpendicular to $\mathbf{M}$, cause off–specular scattering. Due to the mean magnetic field the neutron waves (transmitted and reflected at the interfaces) are birefringent inside each layer in accordance with the Zeeman splitting of the neutron spin states. The spin components of a neutron wave propagate inside a layer with the wave vectors $p_{l\pm} = \{p_0^2 - p_{c\pm}^2\}^{1/2}$ (the eigenvalues of $\hat{p}_l$), where $p_0 = p_0^{f,i}$ is the incoming or scattered wave vector projection onto the normal to the surface, and $p_{c\pm} = p_{cl\pm}$ are the critical wave vectors of the total reflection: $p_{cl\pm}^2 = p_{Nl}^2 \pm p_{Ml}^2$ for that or the other spin component. Those components are transmitted into the layer with the amplitude $t_{l\pm}$, or reflected from its interface with the amplitude $r_{l\pm}$, which are the eigenvalues of the transmission, $\hat{t}_l = t_l + (\mathbf{t}_l\boldsymbol{\sigma})$, and reflection, $\hat{r}_l = r_l + (\mathbf{r}_l\boldsymbol{\sigma})$. Actually, all these amplitudes, including the reflectance $R_\pm = r_{0\pm}$ for the whole multilayer, can easily be found via an ordinary matrix, or Parrat routine, and $t_l = (t_{l+} + t_{l-})/2$, $\mathbf{t}_l = (t_{l+} - t_{l-})\mathbf{b}/2$, $r_l = (r_{l+} + r_{l-})/2$, $\mathbf{r}_l = (r_{l+} - r_{l-})\mathbf{b}/2$, where $\mathbf{b}$ is an unit vector along the mean magnetization.

As soon as the (complex) eigenvalues $R\pm = |R_\pm| \exp(i\chi_\pm^r)$ are found, one can calculate $R = (R_+ + R_-)/2$, $\mathbf{R} = (R_+ - R_-)\mathbf{b}/2$ and the components of the reflectivity matrix $\mathcal{R}_{\pm\pm}^{\alpha\beta} = \mathcal{R}(\pm P_f^\alpha, \pm P_i^\beta)$ and $\mathcal{R}_{\pm\mp}^{\alpha\beta} = \mathcal{R}(\pm P_f^\alpha, \mp P_i^\beta)$ at each of the orthogonal directions of the vector $\mathbf{P}_f$, i.e. at $P_f = P_f^x, P_f^y$, or P_f^z, and at $P_i = P_i^x, P_i^y$, or P_i^z. The results of 36 possible measurements can be collected into the supermatrix $\mathcal{R}_{\mu\nu}^{\alpha\beta}$, with $\{\alpha, \beta\} = \{x, y, z\}$ and μ, ν denote $+$, or $-$. However, in our simple model there are only 3 independent functions, $|R_\pm|$ and $(\chi_+^r - \chi_-^r)$, which can experimentally be determined from this supermatrix, and most

of its elements are interrelated.

Indeed, the quantities $|R_\pm|$ and $(\chi_+^r - \chi_-^r)$ can be found from measurements of the diagonal elements

$$\mathcal{R}_{++}^{yy} = |R_+|^2, \mathcal{R}_{--}^{yy} = |R_-|^2, \tag{108}$$

$$\mathcal{R}_{+-}^{yy} = \mathcal{R}_{-+}^{yy} = 0, \tag{109}$$

$$\mathcal{R}_{++}^{xx(zz)} = \mathcal{R}_{--}^{xx(zz)} = |R_+ + R_-|^2/4, \tag{110}$$

$$\mathcal{R}_{+-}^{xx(zz)} = \mathcal{R}_{-+}^{xx(zz)} = |R_+ - R_-|^2/4, \tag{111}$$

$$|R_+ \pm R_-|^2 = \tag{112}$$

$$|R_+|^2 + |R_-|^2 \pm 2|R_+R_-|\cos(\chi_+^r - \chi_-^r),$$

where it is assumed that $|P_f| = |P_f^y| = 1$ and $|P_i| = |P_i^y| = 1$.

Non–diagonal elements of $\mathcal{R}_{\mu\nu}^{\alpha\beta}$ with $\{\alpha, \beta\} = \{x, z\}$, are as follows:

$$\mathcal{R}_{++}^{\alpha\beta} = \mathcal{R}_{--}^{\alpha\beta} = \mathcal{R}_{+-}^{\beta\alpha} = \mathcal{R}_{-+}^{\alpha\beta}, \tag{113}$$

$$\mathcal{R}_{++}^{zx} = \mathcal{R}_{--}^{zx} = |R_+ - \mathrm{i}R_-|^2/4, \tag{114}$$

$$\mathcal{R}_{+-}^{zx} = \mathcal{R}_{-+}^{zx} = |R_+ + \mathrm{i}R_-|^2/4, \tag{115}$$

$$\mathcal{R}_{++}^{y\alpha} = \mathcal{R}_{+-}^{y\alpha} = \mathcal{R}_{++}^{\alpha y} = \mathcal{R}_{-+}^{\alpha y} = |R_+|^2/2, \tag{116}$$

$$\mathcal{R}_{--}^{y\alpha} = \mathcal{R}_{-+}^{y\alpha} = \mathcal{R}_{--}^{\alpha y} = \mathcal{R}_{+-}^{\alpha y} = |R_-|^2/2. \tag{117}$$

They do not contain an additional information, but can be used to check the consistency of the model anticipating that domains are smaller than the lateral projection of the coherence length. If this is not the case, one cannot use Eqs.(108–117), and the reflectivity must be calculated for each domain, and afterwards the result should be averaged over the domain distribution.

If the domains are not very small then true specular reflection can hardly be discriminated from diffuse scattering within the range of their overlap. As we shall see, the polarization analysis can substantially help to solve this problem. If we assume, that the magnetization of each layer l is decomposed into domains with magnetic moments $\mathbf{M}^l$ tilted at a certain angle ϕ with respect to the mean magnetization directed along the applied field $\mathbf{H}$ (see Fig.1), then the strength of this mean field is $B = H + 4\pi M\cos\phi$, with $M = |\mathbf{M}^l|$. The components $M_x^l = M\sin\phi$ perpendicular to $\mathbf{B}$ are alternating in neighboring domains within each layer, and if the atomic magnetic moments in neighboring layers are coupled antiferromagnetically,

as it happens in GMR systems, then M_x^l components also change sign from layer to layer. Off–specular scattering from such a system of domains is concentrated within the range of $Q_\parallel r_0 \leq 1$ (where r_0 is mean lateral extension of the domains), and has enhancement factor for $q_z d \approx \pi(2n+1)$, where q_z is the wave vector transfer component normal to the surface, d is the multilayer period, and n is integer number.

In the Born approximation (BA) the magnetic scattering operator reads: $\hat{F}_l^{fi} = (\mathbf{F}_l^{fi}\boldsymbol{\sigma})$, where $\mathbf{F}_l^{fi} = b_M \mathcal{F}_M(\mathbf{q})\mathbf{m}_\perp$, b_M is the magnetic scattering length density, $\mathcal{F}_M(\mathbf{q}) = \mathcal{F}_\parallel(\mathbf{q}_\parallel)G_l(q_z)$ is the domain form factor with its lateral, $\mathcal{F}_\parallel$, and transverse, $G_l(q_z)$, components, $\mathbf{m}_{l\perp} = \mathbf{m}_l - \mathbf{e}(\mathbf{e}\mathbf{m}_l)$ is the component of the vector $\mathbf{m}_l = \mathbf{M}_l/M$ perpendicular to the momentum transfer, and $\mathbf{e} = \mathbf{q}/|\mathbf{q}|$. At low angles of incidence and scattering this vector is almost orthogonal to the surface, and thus, to the vector $\mathbf{m}_l$. Then, in our model $\mathbf{m}_{l\perp} \approx \mathbf{m}_l$ is directed along with (or opposite to) the X–axis.

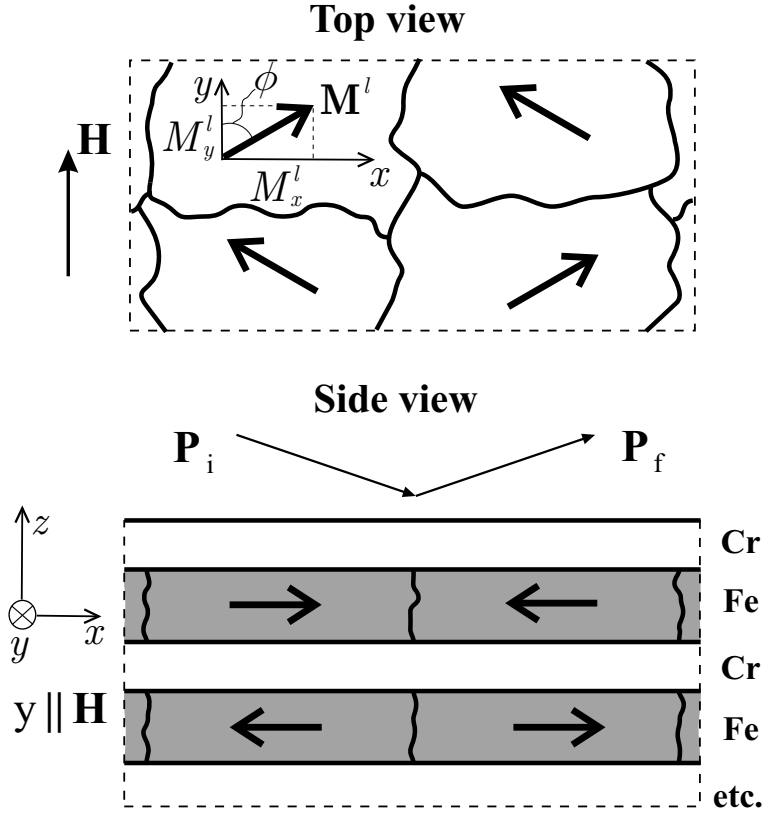

Figure 1: Sketch of the domain magnetization (thick arrows) arrangement of the [[Cr(8.1 Å)/^{57}Fe (67.5 Å)]×12]/Al_2O_3 multilayer.

However, BA is invalid at the angles so low, that the reflection from the mean potential is sufficiently strong. Then, one should take into account refraction effects and the scattering

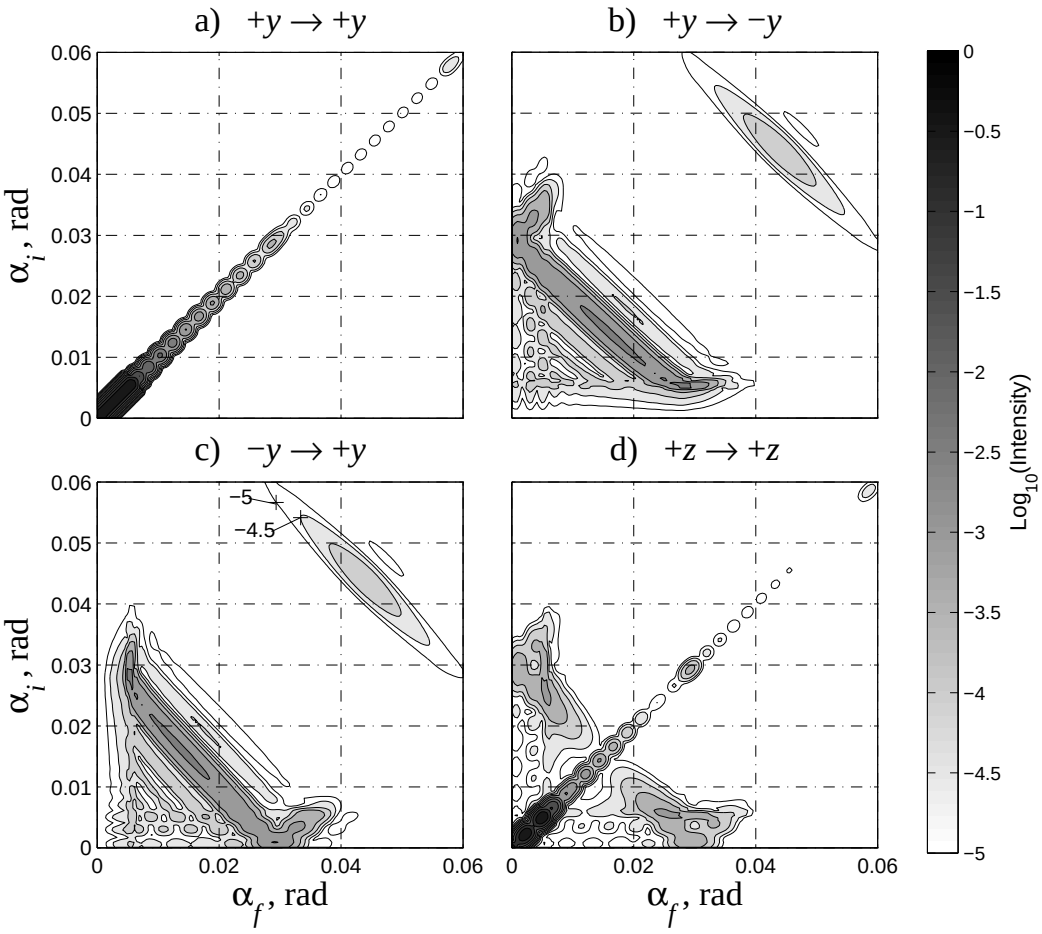

Figure 2: Intensity distribution of: a-c) specular reflection (non–spin–flip) and off–specular scattering (spin–flip) for polarization along the field; d) non–spin–flip reflection and scattering polarization perpendicular to the field, calculated for the model in Fig.1

of the waves reflected from the interfaces. This was done above in the framework of the Distorted Wave BA (DWBA), and the result for each layer l looks as follows:

$$\hat{F}_{fi} = \hat{t}_f \hat{F}^{tt} \hat{t}_i + \hat{t}_f \hat{F}^{tr} \hat{r}_i + \hat{r}_f \hat{F}^{rt} \hat{t}_i + \hat{r}_f \hat{F}^{rr} \hat{r}_i. \tag{118}$$

Beyond BA $\hat{F}_l^{fi}$ is not anymore a function of only the momentum transfer, but depends on each variable, the incident and scattered wave vectors, separately. The vector $\mathbf{F}_l$ is not proportional to $\mathbf{m}_{l\perp}$, but receives also the components perpendicular to this vector. For our model $\mathbf{F}_l = \mathbf{F}_l^{fi}$ has, however, only two components:

$$F_x^{\tau\rho} = \tfrac{b_M}{2}(G_{+-}^{\tau\rho} + G_{-+}^{\tau\rho})\mathcal{F}_\parallel(\mathbf{q}_\parallel), \tag{119}$$

$$F_z^{\tau\rho} = \tfrac{\mathrm{i}b_M}{2}(G_{+-}^{\tau\rho} - G_{-+}^{\tau\rho})\mathcal{F}_\parallel(\mathbf{q}_\parallel). \tag{120}$$

Here $F_{x(z)}^{\tau\rho}$ are the linear combinations of the transverse form–factors $G_{\mu\nu}^{\tau\rho}$ with $\{\tau,\rho\} = \{t,r\}$:

$$G^{tt}_{\mu\nu} = \{e^{\mathrm{i}(p^f_{l\mu}+p^i_{l\nu})a_l} - 1\}/\mathrm{i}(p^f_{l\mu} + p^i_{l\nu}), \tag{121}$$

$$G^{tr}_{\mu\nu} = \{e^{\mathrm{i}(p^f_{l\mu}-p^i_{l\nu})a_l} - 1\}/\mathrm{i}(p^f_{l\mu} - p^i_{l\nu}), \tag{122}$$

$$G^{rt}_{\mu\nu} = -\{e^{-\mathrm{i}(p^f_{l\mu}-p^i_{l\nu})a_l} - 1\}/\mathrm{i}(p^f_{l\mu} - p^i_{l\nu}), \tag{123}$$

$$G^{rr}_{\mu\nu} = -\{e^{-\mathrm{i}(p^f_{l\mu}+p^i_{l\nu})a_l} - 1\}/\mathrm{i}(p^f_{l\mu} + p^i_{l\nu}), \tag{124}$$

where a_l is a layer thickness.

It is important to note that scattering in our model is always associated with transition between different spin states denoted by $\{\mu, \nu\} = \{+, -\}$, Therefore the functions $G^{tt}_{\mu\nu}$ and $G^{rr}_{\mu\nu}$ depend on corresponding "ordinary" wave vector transfers $q^z_{\mu\nu} = p^f_\mu + p^i_\nu$, while the functions $G^{tr}_{\mu\nu}$ and $G^{rt}_{\mu\nu}$ depend on the "anomalous" ones: $\tilde{q}^z_{\mu\nu} = p^f_\mu - p^i_\nu$.

Use of Eqs.(118–124) yields a general equation for the scattering cross sections:

$$\tfrac{d\sigma}{d\Omega}^{yy}_{++} = \tfrac{d\sigma}{d\Omega}^{yy}_{--} = 0, \tag{125}$$

$$\tfrac{d\sigma}{d\Omega}^{yy}_{+-} = |F_x - \mathrm{i}F_z|^2, \tag{126}$$

$$\tfrac{d\sigma}{d\Omega}^{yy}_{-+} = |F_x + \mathrm{i}F_z|^2, \tag{127}$$

$$\tfrac{d\sigma}{d\Omega}^{xx(zz)}_{++} = \tfrac{d\sigma}{d\Omega}^{xx(zz)}_{--} = |F_{x(z)}|^2, \tag{128}$$

$$\tfrac{d\sigma}{d\Omega}^{xx(zz)}_{+-} = \tfrac{d\sigma}{d\Omega}^{xx(zz)}_{-+} = |F_{z(x)}|^2. \tag{129}$$

From these equations it follows that, if at polarization along the field (see, Fig.2a) off–specular scattering is not detected in non–spin–flip channel, but is found in spin–flip channels (see Figs.2b,c), then one still needs to accomplish a set of additional measurements in order to obtain all possible information on the source of scattering. These set must include the experiment with the polarization perpendicular to the mean magnetization. Indeed, the amplitudes $F_{x(z)} = |F_{x(z)}| \exp(i\chi_{x(z)})$ are complex functions and the model is characterized by two absolute values $|F_{x(z)}|$ and by two phases $\chi_{x(z)}$. In accordance with general principles, both of the phases cannot be determined, but the phase shift $(\chi_x - \chi_z)$ can be found. However, this is impossible to do using only Eqs.(125–127), and one needs to employ one of Eqs.(128,129).

All the other (nondiagonal) components of the scattering cross section supermatrix $(d\sigma/d\Omega)^{\alpha\beta}_{\mu\nu}$ do not contain new information on the domain model under consideration. If either $\mathbf{P}_i$, or/and $\mathbf{P}_f$ is directed perpendicular to the field, i.e. $\{\alpha, \beta\} = \{x, z\}$, then:

$$\tfrac{d\sigma}{d\Omega}^{\alpha\beta}_{++} = \tfrac{d\sigma}{d\Omega}^{\alpha\beta}_{--} = |F_x + F_z|^2/2, \tag{130}$$

$$\frac{d\sigma}{d\Omega}^{\alpha\beta}_{+-} = \frac{d\sigma}{d\Omega}^{\alpha\beta}_{-+} = |F_x - F_z|^2/2. \tag{131}$$

$$\frac{d\sigma}{d\Omega}^{\alpha y}_{++} = \frac{d\sigma}{d\Omega}^{\alpha y}_{-+} = \frac{d\sigma}{d\Omega}^{y\alpha}_{--} = \frac{d\sigma}{d\Omega}^{y\alpha}_{-+} = |F_x + \mathrm{i}F_z|^2/2, \tag{132}$$

$$\frac{d\sigma}{d\Omega}^{\alpha y}_{--} = \frac{d\sigma}{d\Omega}^{\alpha y}_{+-} = \frac{d\sigma}{d\Omega}^{y\alpha}_{++} = \frac{d\sigma}{d\Omega}^{y\alpha}_{+-} = |F_x - \mathrm{i}F_z|^2/2. \tag{133}$$

Some examples of the numerical results simulating the experimental observations in [6] are depicted in Figs.2a-c, where the intensity distribution is plotted as a function of the incident angle α_i and the angle of scattering α_f ($p_0^{f,i} = (2\pi/\lambda)\sin\alpha^{f,i}$ and λ is the neutron wave length). In those experiments no off–specular scattering was detected at the incoming and outgoing polarizations directed along with (similar Fig.2a), or opposite (not shown) to the field. On the contrary, spin–flip reflectivities $\mathcal{R}^{yy}_{+-(-+)} = 0$, while off–specular scattering is rather strong, and the intensity distribution in Figs.2b,c reveal a number of remarkable features. Thus, one can clearly see two antiferromagnetic Bragg sheets along which $(p^i_{\pm} + p^f_{\mp})d \approx \pi, 3\pi$, and a set of low intensity sheets running parallel the Bragg ones. The distance between them is determined by the total thickness of the system.

The other prominent property of Figs.2b,c is that the intensity distribution is quite asymmetric. This is due to the asymmetry in the spin–flip scattering amplitude F_z with respect to interchange of the incident and outgoing wave numbers. It is important to remind, that in BA the amplitudes are real functions of the wave vector transfer. This, however, does not hold for DWBA, which takes into account the fact, that the refraction effect for the incoming wave (positive spin projection) is higher, than that for the scattered one, if its spin projection onto the field direction is negative. The effect is mostly pronounced close to the total reflection, while at higher wave vector transfer the symmetry is almost completely restored. The results is Fig.2c are complementary to those in Fig.2b and show, that interchange P^y_f with P^y_i is equivalent with interchange p^f_0 with p^i_0, as follows from the reciprocity principle.

The other effect of DWBA seen in Figs.2b,c is manifested by a short "anomalous" Bragg sheet running perpendicular to the "ordinary" ones, and positioned at $(p^+_i - p^-_f)d \approx \pi$. It arises due to the scattering of the waves reflected from the interfaces. It has appreciable intensity only in the range of strong reflection and is seen in Fig.2b only at low angles of exit. The other process, i.e. reflection of the waves scattered from domains, is rather weak.

At low angles of exit, one can also see some modulation of the intensity which is due to the interference of the fringes running parallel to the "ordinary" and "anomalous" Bragg sheets.

The intensity distribution in Fig.2d is, in contrast to that in Fig.2b,c is rather symmetrical and contains both specular and off–specular components. However, diffuse scattering at the position of specular reflection is heavily suppressed and does not interfere with the reflection process. Indeed, from Eq.(129, 120) it follows that in this case non–spin–flip diffuse scattering cross section is due to the virtual transitions between two spin states However at $p_0^i = p_0^f$ this processes are absolutely equivalent, exactly compensate each other, and $F_l^z = 0$. The off–specular scattering is concentrated close to the range of the total reflection with respect to the incidence, or scattering, while it becomes invisible in the range of BA validity.

9.10 Conclusions and Outlook

In summary, we have shown, that presently there exists the theory which allows to analyze specular reflectivity and off–specular scattering from layered systems with any complex arrangement of inter-layer magnetization, as well as exhibiting in-plane magnetic structure. Numerical routine for the modelling of the scattering signal from multilayers with arbitrarily large number of layers and various in-plane magnetic organization is developed on the basis of this theory by E. Kentzinger and soon will be available on the Web site of IFF. It allows to model scattering at any mutual orientations of incident polarization and polarization analysis. This, I hope, will encourage further efforts of U. Rücker on implementation of 3D polarization analysis, which is, as demonstrated in the last section, rather useful for unique solution of the model of magnetic arrangements in multilayers. In particular, even one experiment with the polarization perpendicular to the mean magnetization carried out in addition to the measurements with polarization along the magnetization allows to determine all possible components of the reflectance and the scattering amplitudes for the model of antiferromagnetic domains.

There is still some theoretical problems to be solved. One of them is to account for the optical theorem, which is responsible for the total flux conservation law. This would, however, require to go beyond the first order of DWBA[19].

Acknowledgments

I am happy to use this opportunity to thank S.V. Maleyev, O.Schärpf, Th. Brückel, I. Anderson, V. Lauter-Pasyuk, H.J. Lauter, G.P. Felcher, V. Syromyatnikov,O. Nikonov, V. Derizalazov, E. Kentzinger, U. Rücker and W. Schweika from whom I, indeed, learned a lot during our long and fruitful collaboration on the subject of the Lecture. I am also deeply indebted to many others with whom I have been collaborating on the topic and apologize, if some of the names are not listed here.

References

[1] . S.V. Maleyev, this volume

[2] W. Marshall and S. W. Lovesey, *Theory of thermal neutron scattering*, (Clarendon Press, Oxford, 1971)

[3] C.S. Schneider, C.G. Shull, Phys.Rev. B3 (1971) 830.

[4] L.D. Landau, E.M. Lifshits, *Ouantum Mechanics*, (Pergamon Press, Oxford, 1977).

[5] M. Born and E. Wolf, *Principles of Optics*, (Pergamon Press, Oxford, 1975)

[6] B.P. Toperverg, A. Rühm, W. Donner, H. Dosch, Physica B 267-268 (1999) 198; A. Rühm, B. Toperverg, H. Dosch, Phys. Rev. B 60 (1999) 16073; B.P. Toperverg, Physica B 279 (2001), 160; B. Toperverg, O. Nikonov, V. Lauter-Passyuk, H. Lauter, Physica B 279 (2001), 169; B.P. Toperverg, Appl. Phys A 75 (2002).

[7] B.P. Toperverg, E. Kentzinger, U. Rücker, Th. Brückel, in preparation.

[8] L. G. Parratt, Phys. Rev. **95**, 359 (1954)

[9] R. Günther, W. Donner, B. Toperverg, H. Dosch, Phys. Rev. Lett. 81 (1998) 116

[10] S.K. Sinha, M. Tolan, A. Gibaud, Phys. Rev.B 57 (1998) 2740; C. F. Majkrzak, Physica B 221 (1996) 342.

[11] S.K. Sinha, E.B. Sirota, S. Garoff, H.B. Stanley, Phys. Rev. B **38** (1988) 2297.

[12] W. Hahn, M. Loewenhaupt, G.P Felcher, Y.Y. Huang, S.S. Parkin, J. Appl. Phys. 75 (1994) 3564; J.A. Borchers J.A. Dura, C.F. Majkrzak, S.Y. Hsu, R. Lolee, W.P. Pratt, J. Bass, Physica B 283 (2000) 162.

[13] B.P. Toperverg, G.P. Felcher, V.V. Metlushko, V. Leiner, R. Sibrecht, O. Nikonov, Physica B 283 (2000) 149.

[14] V. Lauter–Pasyuk, H.J. Lauter, B. Toperverg, O. Nikonov, E. Kravtsov, M.A. Milyaev, L. Romashev, V. Ustinov, Physica B 238 (2000) 194; V.G. Syromytnikov, B.P. Toperverg, E. Kentzinger, et al., Physica B 297 (2001) 175; V. Lauter-Passyuk, H.J. Lauter, B. Toperverg, et al., JMMM 226–230 (2001) 1694; H.J. Lauter, V. Lauter-Pasyuk, B.P. Toperverg, et al., Appl. Phys. A 75 (2002); V. Lauter-Pasyuk, H,J. lauter, B.P. Toperverg, L. Romashev, V. Ustinov, Phys. Rev. Lett., submitted.

[15] G.P. Felcher, S. Adenwalla, V.O. de Haan, A.A. Van Well, Nature 377 (1995) 409; Physica B 221 (1996) 494., V.L. Aksenov, Yu. N. Nikitenko, S.V. Kozhevnikov, Physica B 297 (2001) 94.

[16] F. Pfeiffer, V. Leiner, P. Høghøj, I. Anderson, Phys. Rev. Lett. **88** (2002) 055507-1.

[17] G. P. Felcher, R. O. Hilleke, R. K. Crawford, J. Haumann, R. Kleb, and G. Ostrowski, Rev. Sci. Instr. **58**, 609 (1987)

[18] N. Mott, H.S.W. Messey, *T*he Theory of Atomic Collisions, Oxford at the Clarednon press, 1965.

[19] B.P. Toperverg, O. Schärpf, I.S. Anderson, Physica B 276-278 (2000) 954.